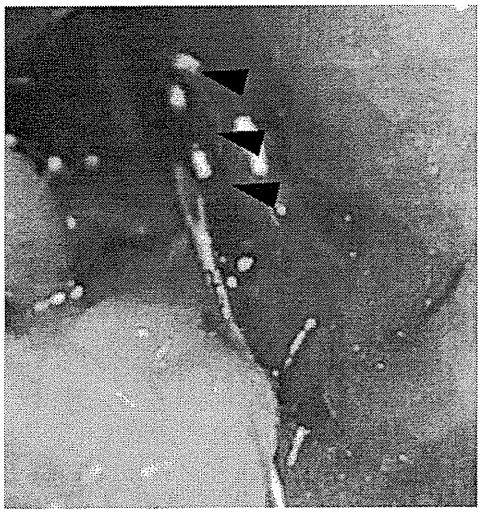

Fig. 1. Intravenous injection via the femoral vein. The skin of the inguinal region is incised, which reveals the left femoral vein. A 35 G needle is inserted into the femoral vein (arrowheads).

(0.5 mg/kg) (Banyu Co., Inc., Tokyo, Japan) in 40 μL of phosphate-buffered saline (PBS) was injected IV 24 h before the HI insult in the first group (i.e., Dex-IV group; $n = 9$) and injected intraperitoneally (IP) in the second group (i.e., Dex-IP group; $n = 8$). *MK-801 cohort*: according to reports showing its neuroprotective effects [28], MK-801 (0.5 mg/kg) (Sigma–Aldrich, St Louis, MO, USA) in 40 μL of PBS was injected IV immediately after the HI insult for the first group (i.e., MK-801-IV group; $n = 9$) and injected IP for the second group (i.e., MK-801-IP group; $n = 9$). The vehicle (PBS) was injected IV (i.e., PBS-IV group) 24 h before the HI insult for the control group ($n = 8$) in the dexamethasone cohort and at 0 h after the HI insult for the control group ($n = 12$) in the MK-801 cohort.

2.4. Evaluations of drug efficacy

In the dexamethasone and MK-801 cohorts, animals were deeply anesthetized, perfused intracardially, and fixed 7 days after the HI insult. In this model, 7 days post-insult is the most common time-point for the evaluation of brain injuries, because the majority of the injury-associated processes have been completed [29,30]. The brain of each animal was removed and coronally sectioned into 1-mm slices. The hemispheric brain volume of each pup was estimated by summing the hemispheric area of the brain slices and multiplying the sum by the section interval thickness as previously described [26,31]. Neuropathological injury was evaluated using hematoxylin–eosin-stained sections from four brain regions: the cortex, striatum, hippocampus, and thalamus. We used a previously established system to evaluate neuropathological injury [32]. Neuropathological injury in the cerebral cortex was scored on a scale ranging from 0 to 4 points (0 = no injury; 4 = extensive confluent infarction), whereas neuropathological injury in the hippocampus, striatum, and thalamus was scored on a scale ranging from 0 to 6 points. The total injury score is the sum of the ratings from all four brain regions (ranging from 0 to 22 points). The investigators evaluating the injuries were blinded as to the experimental group. Immunohistochemical analyses were performed to evaluate neuronal survival or apoptotic cell death using paraffin-embedded brain slices cut into 5-μm sections. Surviving neurons and apoptotic cells were stained with anti-mouse antibodies to NeuN (1:500, Millipore, Bedford, MA, USA) and to cleaved caspase-3 (1:800, Cell Signaling Technology, Inc., Beverly, MA, USA), respectively. After treatment with secondary antibodies, the cells were visualized with 0.5% diaminobenzidine (Wako Pure Chemical Industries, Osaka, Japan) and counterstained with hematoxylin. The total NeuN-positive area was measured automatically using image processing software (WinROOF, Mitani Co. Ltd., Tokyo, Japan), and the number of cleaved caspase-3 positive cells was manually counted in three slices per animal. The average density of NeuN positive cells, and of cleaved caspase-3 positive cells, was calculated for the whole hemisphere.

2.5. Administration of green fluorescent protein-expressing MSCs and MNCs

Bone marrow cells were isolated by flushing out the femoral and tibial cavities of green fluorescent protein (GFP)-expressing Lewis rats (Institute of Laboratory Animals, Kyoto University, Kyoto, Japan) with PBS. *MSC cohort*: the MSCs were prepared as previously described [33]. In brief, bone marrow cells were plated onto 10-cm dishes in a complete culture medium: α-MEM (Invitrogen, Carlsbad, CA, USA) supplemented with 10% FBS (Thermo Fisher Scientific Inc., Waltham, MA, USA), 100 U/mL penicillin, and 100 μg/mL streptomycin (Invitrogen). Five days after plating, the nonadherent cells were removed, and the adherent cells (i.e., MSCs) were further propagated for 4–5 passages. *MNC cohort*: the MNCs were isolated by density gradient centrifugation using Ficoll (GE Healthcare UK Ltd., Amersham Place, England) at 400*g* for 30 min in accordance with the manufacturer's protocol as previously described [34].

Forty-eight hours after the HI insult, we injected GFP-expressing MSCs or MNCs (1×10^5 cells/pup) into the neonatal HIE mice IV (i.e., the IV group) or IP (i.e., the IP group).

2.6. Evaluation of the infused cells

Two or 24 h after the administration of the cells, the pups were euthanized. Their brain, lungs, liver, and

spleen were removed and fixed with 4% paraformaldehyde. The organs were embedded in paraffin blocks and were cut into 2-μm sections. The GFP-positive cells in the organ sections were stained with rabbit anti-GFP polyclonal antibody (1:100, Invitrogen) and anti-rabbit Envision+ system-HRP labeled polymer (Dako Cytomation, Glostrup, Denmark). The cells were visualized with 0.5% diaminobenzidine (Wako Pure Chemical Industries).

2.7. Administration and evaluation of the infused cells in a non-human primate

A 6-years-old male *Macaca fascicularis* (macaque) (body weight, 5 kg) (Keari Co., Ltd. Osaka, Japan) was deeply anesthetized, and the left femoral artery was isolated. Three autothrombins were plugged in the M1 region of the left MCA via a 1.2 French microcatheter. The left MCA was chosen for consistency with the laterality in the mouse HI model. Three days after the occlusion, the macaque was scanned via MRI and an infarct in the left hemisphere was confirmed (Fig. 6A). Seven days after occlusion, bone marrow derived-MNCs were isolated from the bilateral iliac bone of the macaque and were incubated with 100 MBq 2-[^{18}F] fluoro-2-deoxy-D-glucose (^{18}F-FDG) (specific activity, 10 MBq/mL) for 30 min at 37 °C under gentle rolling in serum-free PBS (pH 7.2) and 10 U/mL heparin. To remove excess unbound ^{18}F-FDG, the cells were subjected to a three-step centrifugation and washing process in PBS (7*g*, 27*g*, and 60*g*; each for 120 s). Radioactivity in the supernatant and in the cell pellet was measured with a dose calibrator [35], and 5×10^6 cells radio-labeled with ^{18}F-FDG at 4.5 MBq were injected via the femoral vein of the macaque. Sixty minutes after the cell injection, the radioactivity of the whole body of the macaque was visualized using a three-dimensional positron emission tomography (PET) imaging system (ECAT HR scanner; Siemens-CTI, Knoxville, TN, USA).

2.8. Statistics

All data were expressed as the mean ± the standard error of the mean (SEM). As for the hemispheric volume, comparisons between two parameters were analyzed by Student's *t*-test, and comparisons between three or more groups were analyzed by one-way analysis of variance (ANOVA), followed by the Tukey's test. As for the neuropathological scores and cell distributions, the comparisons between the two parameters were analyzed by the Mann–Whitney *U* test, and the comparisons between three or more groups were analyzed by the Kraskal–Wallis test, followed by the Steel–Dwass test. A *p*-value less than 0.05 was considered statistically significant.

3. Results

3.1. The IV injection via the femoral vein

The success rate of this IV injection procedure was greater than 90% across different operators (data not shown).

3.2. The neuroprotective effects of dexamethasone treatment

Both Dex-IP and Dex-IV significantly ameliorated hemispheric volume loss as compared to PBS-IV (Dex-IP, 3.5 ± 0.9% and Dex-IV, 7.7 ± 1.7% vs. PBS-IV, 16.9 ± 3.2%) (Fig. 2A). Injury to the cortex and hippocampus was also significantly ameliorated by either Dex-IP or Dex-IV, leading to a reduced total injury score compared to PBS-IV (Fig. 2B). Dex-IP or Dex IV also reduced damage to the striatum, although the injury score decrease was only significant for Dex-IP compared to PBS-IV. Despite differences when compared to PBS-IV, there was no significant difference between the injury scores of Dex-IP compared to Dex-IV (Fig. 2B). Neither the ipsilateral/contralateral ratio of the NeuN positive area nor the ratio of cleaved caspase-3 positive cells showed a difference between Dex-IP and Dex-IV (NeuN, Dex-IP, 0.9 ± 0.1 and Dex-IV, 0.8 ± 0.1; cleaved caspase-3, Dex-IP, 1.4 ± 0.2 and Dex-IV, 1.9 ± 1.0, $n = 4$–5) (Fig. 2C and D). Collectively, these results reveal that Dex-IP and Dex-IV treatments result in nearly equal neuroprotective effects.

3.3. The neuroprotective effects of MK-801 treatment

Cerebral hemispheric volume loss was significantly ameliorated by MK-801-IP but not by MK-801-IV compared to PBS-IV (MK-801-IP, 10.2 ± 2.9% and MK-801-IV, 28.6 ± 7.6% vs. PBS-IV, 32.8 ± 5.5%) (Fig. 3A). Similarly, neuropathological injury scores for the striatum were significantly reduced by MK-801-IP but not MK-801-IV compared to PBS-IV. Neither MK-801-IP nor MK-801-IV produced statistically significant neuroprotection in the other regions of the brain or in the total score (Fig. 3B). The ipsilateral/contralateral ratio of the NeuN positive area, which is indicative of surviving neurons, was significantly higher in MK-801-IP (1.0 ± 0.1) than in MK-801-IV (0.7 ± 0.1) ($n = 9$ in each group) (Fig. 3C). The ipsilateral/contralateral ratio of the cleaved caspase-3 positive cells, which is indicative of apoptotic cell death, was significantly lower in MK-801-IP (1.2 ± 1.1) than in MK-801-IV (3.2 ± 0.9) ($n = 9$ in each group) (Fig. 3D). Collectively, MK-801-IP exerted neuroprotective effects whereas MK-801-IV did not.

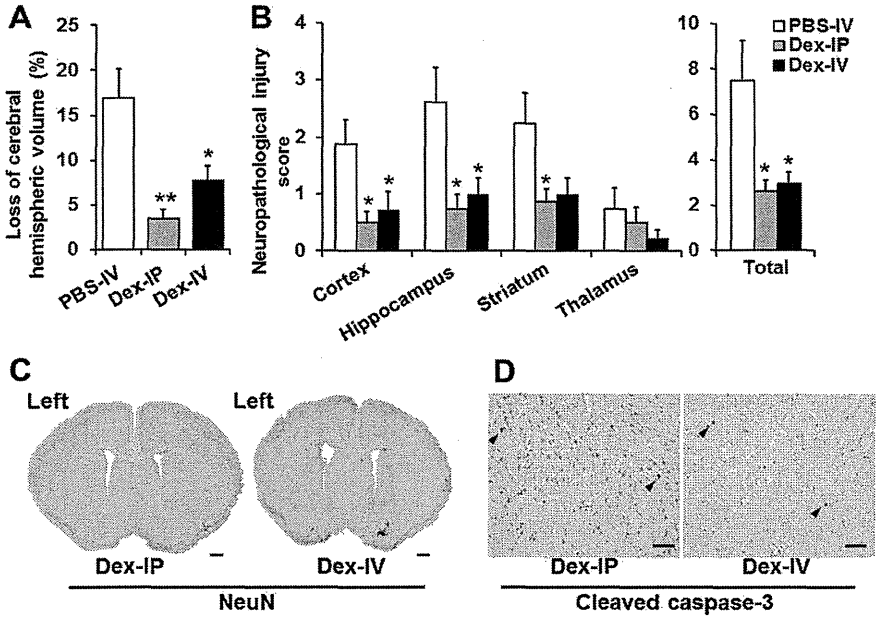

Fig. 2. The neuroprotective effects of intravenously or intraperitoneally injected dexamethasone in neonatal mice with hypoxic–ischemic encephalopathy. (A) The loss of ipsilateral cerebral hemispheric volume is calculated as follows: ((contralateral volume – ipsilateral volume)/contralateral volume × 100%). (B) The neuropathological injury scores of the cortex, hippocampus, striatum, and thalamus (0 indicates no injury; the cortex is scored 0–4, and the hippocampus, striatum, and thalamus are each scored 0–6). The total injury score is the sum of the scores for the four brain regions. Dex-IP and PBS-IV groups, $n = 8$; Dex-IV group, $n = 9$. $^{*}p < 0.05$ vs. PBS-IV. $^{**}p < 0.01$ vs. PBS-IV. (C) Representative images of the coronal brain sections stained with NeuN. The scale bars represent 500 μm. (D) Representative images of the cleaved caspase-3 expressing cells in the ipsilateral cerebral hemisphere. The scale bars represent 50 μm. *Abbreviations:* Dex-IP, mouse pups intraperitoneally injected with dexamethasone; Dex-IV, mouse pups intravenously injected with dexamethasone; PBS-IV, mouse pups intravenously injected with phosphate-buffered saline.

3.4. The distribution of administered MSCs

The mean diameter of the MSCs was 21.5 ± 0.6 μm. At 2 h after administration, a remarkable accumulation of infused MSCs was observed in the lungs among the four organs examined in the MSC-IV group, whereas the cells were evenly detected in the four organs in the MSC-IP group (Fig. 4A and B). The MSC-IV resulted in a significantly higher number of cells in the lungs and the brain than the MSC-IP at 2 h after administration. From 2 h to 24 h after the administration of MSCs, the mean number of infused cells tended to decrease in the IV group but tended to increase in the IP group across each organ, although these temporal changes were not statistically significant, except the significant decrease in the brain in the IV group. At 24 h after administration, no significant differences were observed between the MSC-IV and the MSC-IP groups. A comparison between the ipsilateral cerebral hemisphere and the contralateral cerebral hemisphere revealed no significant difference in the number of transfused cells in either the IP or IV group at either time point (at 2 h after transplant; ipsilateral 10.7 ± 4.7 cells/cm^2 vs. contralateral 8.2 ± 2.2 cells/cm^2 in the IV group, ipsilateral, 3.8 ± 0.7 cells/cm^2 vs. contralateral, 3.7 ± 1.4 cells/cm^2 in the IP group, at 24 h after transfusion; data not shown). We also analyzed the localization of the cells within the brain (e.g., cortex, hippocampus, striatum, thalamus, and white matter) and found no difference between the IV and IP groups in any of the five brain regions (data not shown).

3.5. The distribution of administered MNCs

The mean diameter of MNCs was 7.1 ± 0.6 μm. At 2 h after administration, the MNC-IV resulted in a significantly higher number of cells in the liver, the lungs, and the spleen but not in the brain than the MNC-IP (Fig. 5). From 2 h to 24 h after the administration of MNCs, the mean number of infused cells significantly decreased in the liver and the lungs but remained at the same level in the spleen in the IV group. Only a few cells were detected in any of the four regions in the IP cohort at either time point, and no obvious temporal changes were observed in the number of cells across the organs. At 24 h after the administration, in the spleen, MNC-IV resulted in a significantly higher number of cells compared to the MNC-IP. A comparison between the ipsilateral cerebral hemisphere and the contralateral cerebral hemisphere revealed no significant difference in the number of transfused cells in either the IP or IV group at either time point (data not shown).

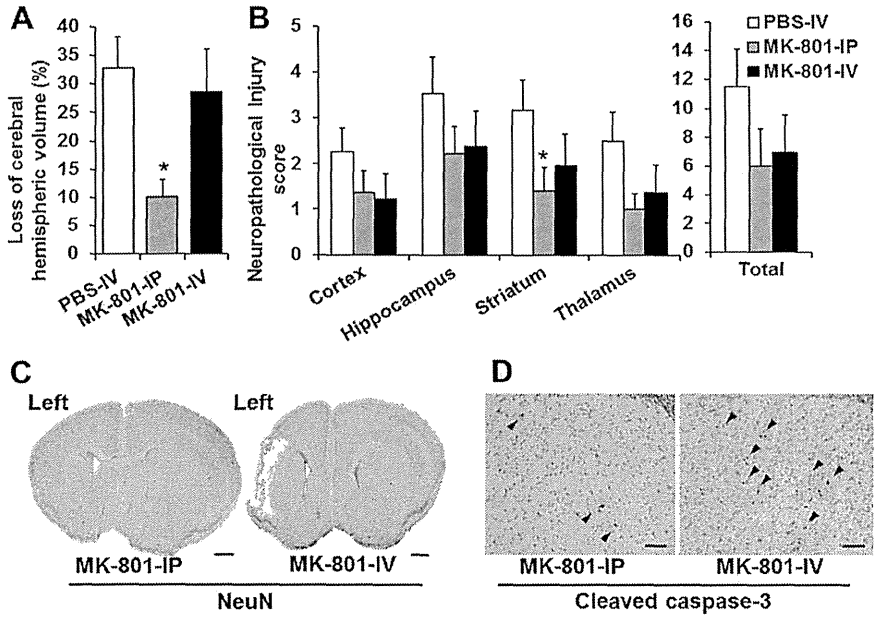

Fig. 3. The neuroprotective effects of intravenously or intraperitoneally injected MK-801 in neonatal mice with hypoxic–ischemic encephalopathy. (A) The loss of ipsilateral cerebral hemispheric volume is calculated as follows: ((contralateral volume − ipsilateral volume)/contralateral volume × 100%). (B) The neuropathological injury scores of the cortex, hippocampus, striatum, and thalamus (0 indicates no injury; the cortex is scored 0–4, and the hippocampus, striatum, and thalamus are each scored 0–6). The total injury score is the sum of the scores for the four brain regions. MK-801-IP and MK-801-IV groups, $n = 9$; PBS-IV group, $n = 12$. $^{*}p < 0.05$ vs. PBS-IV. (C) Representative images of coronal brain sections stained with NeuN. The scale bars represent 500 μm. (D) Representative images of cleaved caspase-3 expressing cells in the ipsilateral cerebral hemisphere. The scale bars represent 50 μm. *Abbreviations:* MK-801-IP, mouse pups intraperitoneally injected with MK-801; MK-801-IV, mouse pups intravenously injected with MK-801; PBS-IV, mouse pups intravenously injected with phosphate-buffered saline.

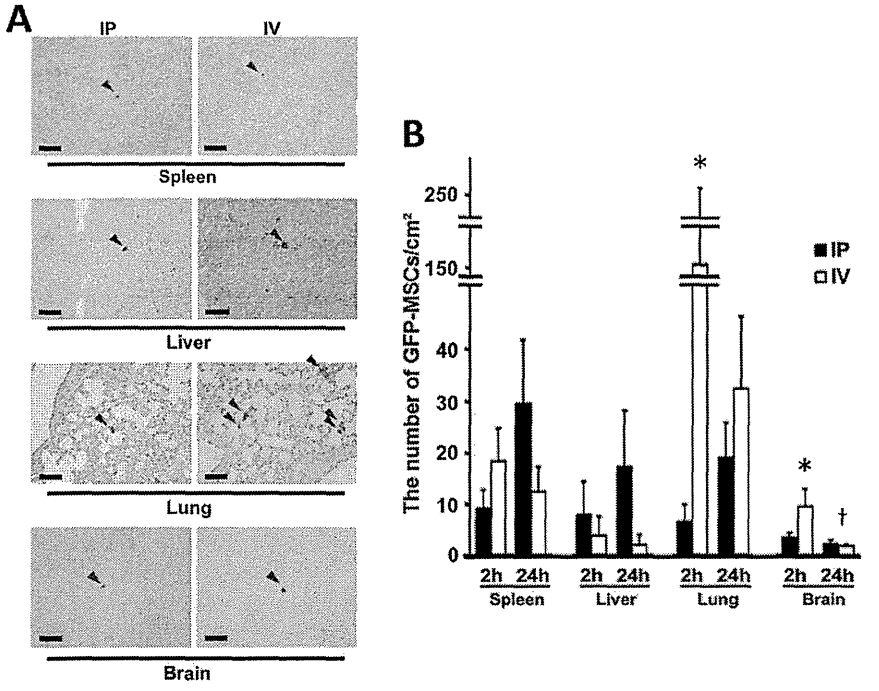

Fig. 4. The distribution of green fluorescent protein (GFP)–positive mesenchymal stem cells (MSCs) intraperitoneally or intravenously injected into neonatal mice with hypoxic-ischemic encephalopathy at 2 h and 24 h after the cell injection. (A) Representative immunohistological staining (i.e., anti-GFP antibody with diaminobenzidine) of the MSCs (arrowheads) in the spleen, liver, lung and brain at 2 h after the cell injection. The scale bar represents 50 μm. (B) Quantitative analysis of MSC distribution at 2 h and 24 h after intraperitoneal (solid bars) and intravenous (open bars) administrations. $n = 10$–13; $^{*}p < 0.05$, vs. IP; $^{\dagger}p < 0.05$, vs. 2 h. *Abbreviations:* IP, intraperitoneal; IV, intravenous.

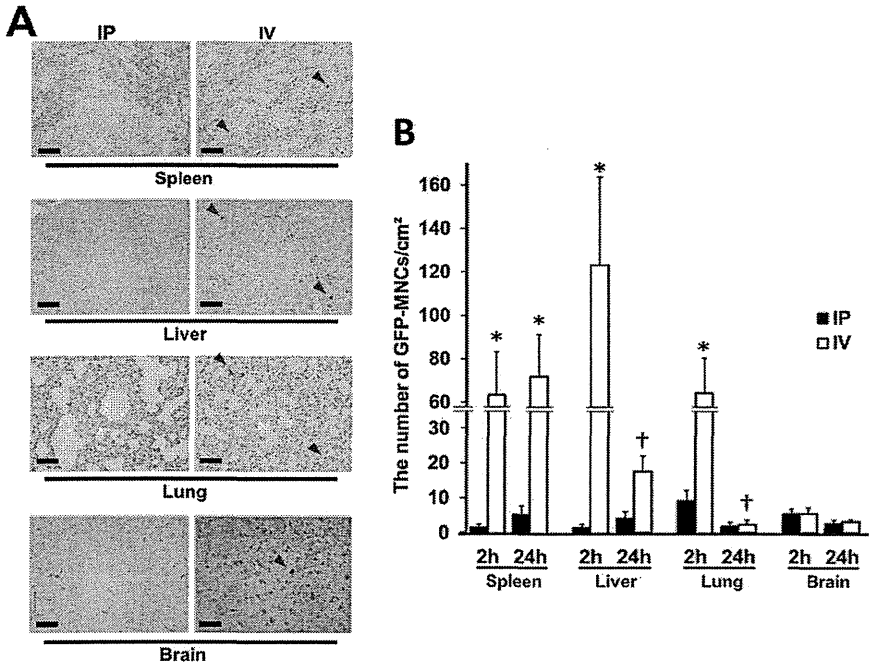

Fig. 5. The distribution of green fluorescent protein (GFP)–positive bone marrow mononuclear cells (MNCs) intraperitoneally or intravenously injected into neonatal mice with hypoxic-ischemic encephalopathy at 2 h and 24 h after the cell injection. (A) Representative immunohistological staining (i.e., anti-GFP antibody with diaminobenzidine) of the MNCs (arrowheads) in the spleen, liver, lung and brain. The scale bar represents 50 μm. (B) Quantitative analysis of MNC distribution at 2 h and 24 h after intraperitoneal (solid bars) and intravenous (open bars) administrations. $n = 8$–9; $^{*}p < 0.05$, vs. IP; $^{\dagger}p < 0.05$, vs. 2 h. *Abbreviations:* IP, intraperitoneal; IV, intravenous.

With regard to the localization of the cells within the brain, no difference was observed between the IV and IP groups (data not shown).

3.6. Distribution of MNCs in a macaque model of stroke

Following permanent MCA occlusion in a macaque, an infarct in the left hemisphere was confirmed at 3 days by MRI (Fig. 6A). At 1 h after the IV administration of MNCs, a PET scan demonstrated that a large number of infused MNCs accumulated in the spleen (9.1 kBq/mL), followed by the liver (2.7 kBq/mL) and the lung (1.4 kBq/mL) (Fig. 6B and C). The accumulation in the brain was weak (0.7 kBq/mL), and no laterality was observed (Fig. 6B and C).

4. Discussion

4.1. A simple and precise IV injection technique in neonatal mice

In the present study, we demonstrated a simple and precise injection technique into the femoral vein in neonatal mice. Three papers have recently described an IV injection technique in neonatal mice [5–7]. In these papers, the superficial temporal vein or jugular vein was the injection site, and the procedure can require two people [6]. Although IV injection in P1–3 mice has been documented in several experiments [36,37], the technique has not been commonly used in experiments with neonatal mice and rats. For example, among the 11 reports on the systemic administration of umbilical cord blood cells in neonatal rodents with HI brain injury in literature, 4 reports used IV injection [38–41] and 7 reports used IP injection [8–14]. All of these reports were on P7 rat pups, and mice pups were not studied in the field. The benefits of our technique are that one person can execute the whole procedure alone and can also confirm that a solution is flowing within a blood vessel.

4.2. Different effects of drug therapies

To examine whether IP injection is comparable to IV injection, we examined the therapeutic effects of two neuroprotective drugs (i.e., dexamethasone and MK-801) in neonatal mice with HIE. To our knowledge, there is no existing report on the use of animal models of brain damage that compares the differences in the therapeutic potency or in the plasma and brain levels after the IV or IP administration of either dexamethasone or MK-801. We demonstrated that the neuroprotective effects of MK-801 were dependent on the administration route, whereas the effects of dexamethasone were not. Dexamethasone (molecular weight,

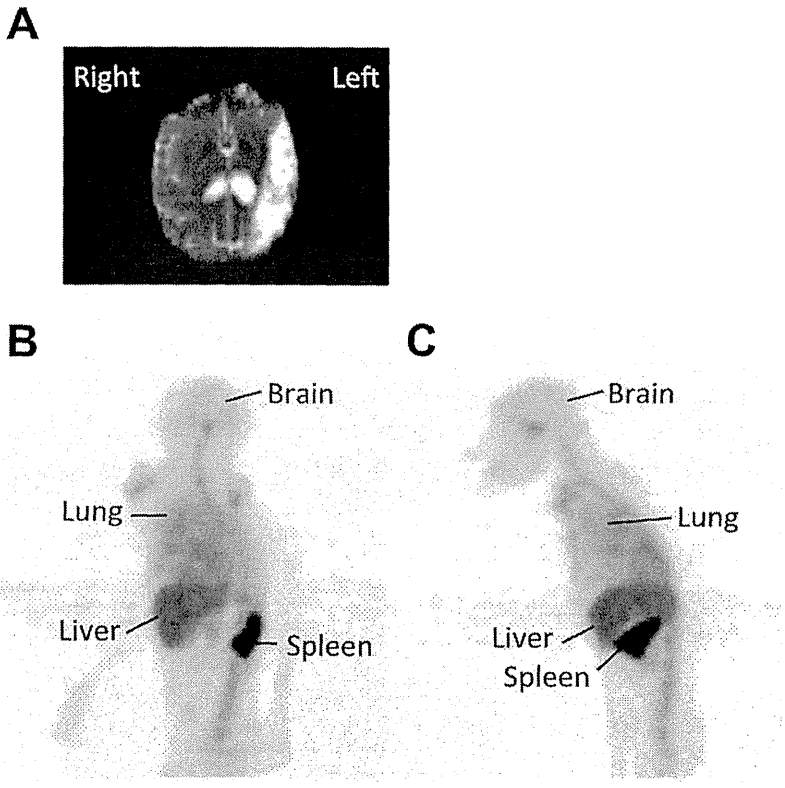

Fig. 6. The distribution of 2-[^{18}F]fluoro-2-deoxy-D-glucose (^{18}F-FDG)-labeled bone marrow derived-mononuclear cells (MNCs) intravenously injected in a macaque model of stroke. (A) Axial T2-weighted image of MRI at 3 days after middle cerebral occlusion (MCAO). The image shows a large infarct in the left hemisphere. (B, C) Positron emission tomography (PET) images at 60 min after the intravenous injection of ^{18}F-FDG-labeled bone marrow derived-MNCs. The black color shows the radioactivity of ^{18}F-FDG-labeled cells. (B) Front elevation image of the macaque. (C) Side elevation image of the macaque.

392.461 g/mol) has a long period of bioactivity, although the plasma level of dexamethasone rapidly decreased after administration [42,43]. The plasma half-life of dexamethasone after IV injection in adult rats is 2.3 h [44]. After IV injection of dexamethasone, rapid accumulation occurs in the adult rat brain, followed by rapid washout. After 10 min and 30 min, 74% and 13% of the concentration observed at 2.5 min remains, respectively [45]. The therapeutic time window of its pretreatment for brain injury is long (e.g., single IP injection at either 6 h or 24 h before HI insult prevents infarction) [27]. Single IP injection at 0 h or 3 h before HI insult does not exert neuroprotection; therefore, the effects of dexamethasone may involve the modification of gene expression [27,43]. Ultimately, differences in pharmacokinetics caused by a different administration route may not have been critical when animals were treated 24 h before the insult with dexamethasone.

MK-801 (molecular weight, 337.37 g/mol) is a non-competitive antagonist of the NMDA-type of excitatory amino acid receptors and enters the brain with no diffusion restriction because of its lipophilic nature [46]. We subsequently used MK-801 to eliminate the local (i.e., intraperitoneal and/or intravascular) and systemic effects that dexamethasone may exert after IV or IP injection. MK-801 reaches maximal concentrations in the adult rat brain within 10–30 min after IP administration with an elimination half-life of 2.05 h [46]. A recent study showed a somewhat delayed time to the maximal concentration in the adult rat brain 40–60 min after IP administration [47]. The MK-801 concentration at 60 min after IV administration in the non-ischemic brain regions of adult rats with permanent MCA occlusion decreases by more than 50% from the level at 15 min [48]. No study has directly compared the pharmacokinetics of MK-801 after IV and IP, but the above-mentioned studies indicate that the brain level of MK-801 may drop faster after IV than after IP administration, although the difference may not be large. Brain ischemia causes a rapid and drastic increase in excitatory amino acids, specifically glutamate, and activation of NMDA receptors [19]. The duration of glutamate accumulation and activation of NMDA receptors is short in models with reperfusion [19], which results in a narrow therapeutic time window of MK-801 activity [19,49,50]. Therefore, a small difference in the duration in which a drug maintains its therapeutic concentration in the brain may make a big difference. Correctively, the

different therapeutic effects of MK-801 observed in the present study may be due to the subtle difference in the pharmacokinetics caused by the different administration routes.

In using a therapeutic agent that has a long bioactivity time such as dexamethasone, the IP route can be used in preclinical studies as an alternative to IV, which is the expected administration route in the clinical setting. By contrast, when using a neuroprotectant that has a short therapeutic time window such as MK-801, it is important to choose the optimal administration route in the preclinical study.

4.3. Different cell distributions

The present study demonstrated that the IV administration of MSCs or MNCs resulted in a significantly higher number of cells accumulating in several organs compared to IP administration. The difference in cell accumulation according to administration route was dependent on the time after the administration, the cell type, and the organ. To our knowledge, only one report has compared the cell distributions after IV and IP administrations in immature animals. The study using the polymerase chain reaction (PCR) for a human-specific gene fragment in neonatal rats with excitatory brain injury showed that human MNCs were detectable at 5 min and up to 2 h after IV administration primarily in the blood, lung, and liver, and only in small amounts in the brain; however, no human MNCs were detected in either the blood or the lungs at any experimental time point from 5 min to 5 days after IP administration [51]. Additionally, that report [51] is the only study that examined the systemic cell distribution in animals with neonatal brain injury. A few studies have examined the differences in the systemic cell distribution after different infusion methods in adult rodents. Gao et al. used the γ camera to detect ^{111}In-oxine-labeled MSCs and demonstrated that the radioactivity accumulated in the lung immediately after IV infusion and primarily in the liver 48 h after IV infusion. After IP infusion, radioactivity was observed in the liver, spleen, kidneys, and lungs in small amounts [52].

In the short term, IV administration appears to be more advantageous for conveying donor cells to the brain compared to IP administration; however, studies have shown that the amount of donor cells that reach the brain is limited even after IV administration [41,53], which is supported by our observations. Collectively, although the data are limited, they indicate that donor cell distributions differ depending on the administration route.

In contrast to the aforementioned study [51], several studies on neonatal rats with HI showed that human MNCs were detectable in the cerebral hemisphere at 1 day [11], 2 days [10], 2 weeks [9], and 40 days [8] after IP administration using immunohistochemical staining and 13 days after IP administration using PCR [11]. These studies showed the exclusive distribution of donor cells (MNCs) in the injured hemisphere. By contrast, the present study showed an even distribution of donor cells (MSCs and MNCs) across the ipsilateral and contralateral hemispheres either after IV or IP administration, and this observation is in accordance with a study that used IV administration of MNCs [40] and one that used intracardiac administration of MSCs [54]. In addition to the time after the administration, the cell type, and the organ, detecting the transfused cells may depend on various factors such as the type and intensity of brain injury, the transfused cell dose, species and strain, capillary size, and detection method. With these numerous factors and the temporally changing nature of cell distribution, it may not be appropriate to compare different sets of data obtained under different experimental paradigms.

With respect to the influence that different cell types may cause in the cell distribution, 4% of IV-administered MNCs entered the common carotid arterial, and the rate was markedly lower for MSCs (1/30 of MNCs) in adult rats [55]. Administered cells (MNCs and MSCs) were detected only in the lungs and not in other organs. Studies have shown that the vast majority of IV-administered cells, especially MSCs, are trapped within the lungs at least during the acute phase after administration and that the entrapment depends on the size of the infused cells [55,56]. The mean diameter of adult mouse pulmonary capillaries is approximately 15 μm, and larger cells are consequently trapped within the lung [56]. The mean diameter of MSCs is approximately 20 μm, and the mean diameter of bone marrow derived-MNCs is approximately 7 μm [55,56]. In our observation, in a larger animal such as a macaque with a stroke, IV administration of MNCs resulted in high accumulation of the cells in the liver and spleen, and the distribution in the lung was low, unlike in neonatal mice. Clinical studies with intra-arterial administration of MNCs in patients with ischemic stroke or myocardial infarction demonstrate that MNCs accumulate in the liver and spleen rather than the targeted organ [35,57]. Collectively, the evidence shows that infused cells tend to accumulate in the liver and spleen regardless of the administration route and recipient species. In addition to the donor cell size and host capillary size, other factors may influence the entrapment. For example, MSCs are adhesive cells, whereas MNCs are not adhesive. Blocking cell adhesive molecules reportedly increases pulmonary passage [55].

4.4. Conclusion

The route of administration may influence the effects of drugs. IP injection differs from IV injection with respect to cell distribution after cell transplantation. Therefore, caution should be exercised when translating

data obtained in animal studies using IP administration for use in clinical trials with IV administration. Preclinical studies using IV administration may be necessary before clinical trials when the anticipated administration route is IV, especially for cell-based therapies.

Acknowledgements

This work was supported by the JSPS KAKENHI, Grant No. 24591617. We are grateful to the National BioResource Project in Japan (http://www.anim.med.kyoto-u.ac.jp/NBR/) for providing the rat strain LEW-TgN(CAG-EGFP)1Ys. We would also like to thank Manami Sone and Mari Furuta for their technical assistance.

References

[1] van Handel M, Swaab H, de Vries LS, Jongmans MJ. Long-term cognitive and behavioral consequences of neonatal encephalopathy following perinatal asphyxia: a review. Eur J Pediatr 2007;166:645–54.
[2] Hosono T, Kamo A, Hakotani S, Minato K, Akeno H, Taguchi Y, et al. Effect of hypothermia on motor function of adult rats after neonatal hyperthermic hypoxic–ischemic brain insult. Eur J Appl Physiol 2010;109:35–9.
[3] Gunn AJ, Hoehn T, Hansmann G, Buhrer C, Simbruner G, Yager J, et al. Hypothermia: an evolving treatment for neonatal hypoxic ischemic encephalopathy. Pediatrics 2008;121:648–9 (author reply 649–50).
[4] Hagberg H, Peebles D, Mallard C. Models of white matter injury: comparison of infectious, hypoxic–ischemic, and excitotoxic insults. Ment Retard Dev Disabil Res Rev 2002;8:30–8.
[5] Glascock JJ, Osman EY, Coady TH, Rose FF, Shababi M, Lorson CL. Delivery of therapeutic agents through intracerebroventricular (ICV) and intravenous (IV) injection in mice. J Vis Exp 2011;56:2968.
[6] Kienstra KA, Freysdottir D, Gonzales NM, Hirschi KK. Murine neonatal intravascular injections: modeling newborn disease. J Am Assoc Lab Anim Sci 2007;46:50–4.
[7] Sands MS, Barker JE. Percutaneous intravenous injection in neonatal mice. Lab Anim Sci 1999;49:328–30.
[8] Geissler M, Dinse HR, Neuhoff S, Kreikemeier K, Meier C. Human umbilical cord blood cells restore brain damage induced changes in rat somatosensory cortex. PLoS One 2011;6:e20194.
[9] Meier C, Middelanis J, Wasielewski B, Neuhoff S, Roth-Haerer A, Gantert M, et al. Spastic paresis after perinatal brain damage in rats is reduced by human cord blood mononuclear cells. Pediatr Res 2006;59:244–9.
[10] Pimentel-Coelho PM, Magalhaes ES, Lopes LM, deAzevedo LC, Santiago MF, Mendez-Otero R. Human cord blood transplantation in a neonatal rat model of hypoxic-ischemic brain damage: functional outcome related to neuroprotection in the striatum. Stem Cells Dev 2010;19:351–8.
[11] Rosenkranz K, Kumbruch S, Lebermann K, Marschner K, Jensen A, Dermietzel R, et al. The chemokine SDF-1/CXCL12 contributes to the 'homing' of umbilical cord blood cells to a hypoxic–ischemic lesion in the rat brain. J Neurosci Res 2010;88:1223–33.
[12] Rosenkranz K, Kumbruch S, Tenbusch M, Marcus K, Marschner K, Dermietzel R, et al. Transplantation of human umbilical cord blood cells mediated beneficial effects on apoptosis, angiogenesis and neuronal survival after hypoxic–ischemic brain injury in rats. Cell Tissue Res 2012;348:429–38.
[13] Rosenkranz K, Tenbusch M, May C, Marcus K, Meier C. Changes in Interleukin-1 alpha serum levels after transplantation of umbilical cord blood cells in a model of perinatal hypoxic–ischemic brain damage. Ann Anat 2013;195:122–7.
[14] Wasielewski B, Jensen A, Roth-Harer A, Dermietzel R, Meier C. Neuroglial activation and Cx43 expression are reduced upon transplantation of human umbilical cord blood cells after perinatal hypoxic–ischemic injury. Brain Res 2012;1487:39–53.
[15] Castillo-Melendez M, Yawno T, Jenkin G, Miller SL. Stem cell therapy to protect and repair the developing brain: a review of mechanisms of action of cord blood and amnion epithelial derived cells. Front Neurosci 2013;7:194.
[16] Ikeda T, Mishima K, Yoshikawa T, Iwasaki K, Fujiwara M, Xia YX, et al. Dexamethasone prevents long-lasting learning impairment following neonatal hypoxic–ischemic brain insult in rats. Behav Brain Res 2002;136:161–70.
[17] Tuor UI, Simone CS, Barks JD, Post M. Dexamethasone prevents cerebral infarction without affecting cerebral blood flow in neonatal rats. Stroke 1993;24:452–7.
[18] Chumas PD, Del Bigio MR, Drake JM, Tuor UI. A comparison of the protective effect of dexamethasone to other potential prophylactic agents in a neonatal rat model of cerebral hypoxia–ischemia. J Neurosurg 1993;79:414–20.
[19] Margaill I, Parmentier S, Callebert J, Allix M, Boulu RG, Plotkine M. Short therapeutic window for MK-801 in transient focal cerebral ischemia in normotensive rats. J Cereb Blood Flow Metab 1996;16:107–13.
[20] Park CK, Nehls DG, Graham DI, Teasdale GM, McCulloch J. The glutamate antagonist MK-801 reduces focal ischemic brain damage in the rat. Ann Neurol 1988;24:543–51.
[21] Jiang Y, Jahagirdar BN, Reinhardt RL, Schwartz RE, Keene CD, Ortiz-Gonzalez XR, et al. Pluripotency of mesenchymal stem cells derived from adult marrow. Nature 2002;418:41–9.
[22] Haynesworth SE, Baber MA, Caplan AI. Cytokine expression by human marrow-derived mesenchymal progenitor cells in vitro: effects of dexamethasone and IL-1 alpha. J Cell Physiol 1996;166:585–92.
[23] Wakitani S, Saito T, Caplan AI. Myogenic cells derived from rat bone marrow mesenchymal stem cells exposed to 5-azacytidine. Muscle Nerve 1995;18:1417–26.
[24] Mareschi K, Ferrero I, Rustichelli D, Aschero S, Gammaitoni L, Aglietta M, et al. Expansion of mesenchymal stem cells isolated from pediatric and adult donor bone marrow. J Cell Biochem 2006;97:744–54.
[25] Brehm M, Zeus T, Strauer BE. Stem cells – clinical application and perspectives. Herz 2002;27:611–20.
[26] Ohshima M, Tsuji M, Taguchi A, Kasahara Y, Ikeda T. Cerebral blood flow during reperfusion predicts later brain damage in a mouse and a rat model of neonatal hypoxic–ischemic encephalopathy. Exp Neurol 2012;233:481–9.
[27] Tuor UI. Dexamethasone and the prevention of neonatal hypoxic–ischemic brain damage. Ann NY Acad Sci 1995;765:179–95 (discussion 196–7).
[28] Hagberg H, Gilland E, Diemer NH, Andine P. Hypoxia–ischemia in the neonatal rat brain: histopathology after post-treatment with nmda and non-nmda receptor antagonists. Biol Neonate 1994;66:205–13.
[29] Han BH, DeMattos RB, Dugan LL, Kim-Han JS, Brendza RP, Fryer JD, et al. Clusterin contributes to caspase-3-independent brain injury following neonatal hypoxia–ischemia. Nat Med 2001;7:338–43.
[30] Sabir H, Scull-Brown E, Liu X, Thoresen M. Immediate hypothermia is not neuroprotective after severe hypoxia–ischemia and is deleterious when delayed by 12 hours in neonatal rats. Stroke 2012;43:3364–70.

[31] Tsuji M, Taguchi A, Ohshima M, Kasahara Y, Ikeda T. Progesterone and allopregnanolone exacerbate hypoxic-ischemic brain injury in immature rats. Exp Neurol 2012;233:214–20.
[32] Tsuji M, Wilson MA, Lange MS, Johnston MV. Minocycline worsens hypoxic-ischemic brain injury in a neonatal mouse model. Exp Neurol 2004;189:58–65.
[33] Ohnishi S, Yanagawa B, Tanaka K, Miyahara Y, Obata H, Kataoka M, et al. Transplantation of mesenchymal stem cells attenuates myocardial injury and dysfunction in a rat model of acute myocarditis. J Mol Cell Cardiol 2007;42:88–97.
[34] Nakano-Doi A, Nakagomi T, Fujikawa M, Nakagomi N, Kubo S, Lu S, et al. Bone marrow mononuclear cells promote proliferation of endogenous neural stem cells through vascular niches after cerebral infarction. Stem Cells 2010;28:1292–302.
[35] Hofmann M, Wollert KC, Meyer GP, Menke A, Arseniev L, Hertenstein B, et al. Monitoring of bone marrow cell homing into the infarcted human myocardium. Circulation 2005;111:2198–202.
[36] Daly TM, Vogler C, Levy B, Haskins ME, Sands MS. Neonatal gene transfer leads to widespread correction of pathology in a murine model of lysosomal storage disease. Proc Natl Acad Sci USA 1999;96:2296–300.
[37] Carbonaro DA, Jin X, Petersen D, Wang X, Dorey F, Kil KS, et al. In vivo transduction by intravenous injection of a lentiviral vector expressing human ADA into neonatal ADA gene knockout mice: a novel form of enzyme replacement therapy for ADA deficiency. Mol Ther 2006;13:1110–20.
[38] Bae SH, Kong TH, Lee HS, Kim KS, Hong KS, Chopp M, et al. Long-lasting paracrine effects of human cord blood cells on damaged neocortex in an animal model of cerebral palsy. Cell Transplant 2012;21:2497–515.
[39] de Paula S, Greggio S, Marinowic DR, Machado DC, DaCosta JC. The dose-response effect of acute intravenous transplantation of human umbilical cord blood cells on brain damage and spatial memory deficits in neonatal hypoxia–ischemia. Neuroscience 2012;210:431–41.
[40] de Paula S, Vitola AS, Greggio S, de Paula D, Mello PB, Lubianca JM, et al. Hemispheric brain injury and behavioral deficits induced by severe neonatal hypoxia–ischemia in rats are not attenuated by intravenous administration of human umbilical cord blood cells. Pediatr Res 2009;65:631–5.
[41] Yasuhara T, Hara K, Maki M, Xu L, Yu G, Ali MM, et al. Mannitol facilitates neurotrophic factor up-regulation and behavioural recovery in neonatal hypoxic–ischaemic rats with human umbilical cord blood grafts. J Cell Mol Med 2010;14:914–21.
[42] Al Katheeri NA, Wasfi IA, Lambert M, Saeed A. Pharmacokinetics and pharmacodynamics of dexamethasone after intravenous administration in camels: effect of dose. Vet Res Commun 2004;28:525–42.
[43] Earp JC, Dubois DC, Molano DS, Pyszczynski NA, Almon RR, Jusko WJ. Modeling corticosteroid effects in a rat model of rheumatoid arthritis II: mechanistic pharmacodynamic model for dexamethasone effects in Lewis rats with collagen-induced arthritis. J Pharmacol Exp Ther 2008;326:546–54.
[44] Samtani MN, Jusko WJ. Comparison of dexamethasone pharmacokinetics in female rats after intravenous and intramuscular administration. Biopharm Drug Dispos 2005;26:85–91.
[45] Kostron H, Fischer J. Regional, cellular, and subcellular distribution of [^{3}H]dexamethasone in rat brain edema. Surg Neurol 1983;20:48–54.
[46] Vezzani A, Serafini R, Stasi MA, Caccia S, Conti I, Tridico RV, et al. Kinetics of MK-801 and its effect on quinolinic acid-induced seizures and neurotoxicity in rats. J Pharmacol Exp Ther 1989;249:278–83.
[47] Wegener N, Nagel J, Gross R, Chambon C, Greco S, Pietraszek M, et al. Evaluation of brain pharmacokinetics of (+)MK-801 in relation to behaviour. Neurosci Lett 2011;503:68–72.
[48] Wallace MC, Teasdale GM, McCulloch J. Autoradiographic analysis of ^{3}H-MK-801 (dizocilpine) in vivo uptake and in vitro binding after focal cerebral ischemia in the rat. J Neurosurg 1992;76:127–33.
[49] Hattori H, Morin AM, Schwartz PH, Fujikawa DG, Wasterlain CG. Posthypoxic treatment with MK-801 reduces hypoxic–ischemic damage in the neonatal rat. Neurology 1989;39:713–8.
[50] McDonald JW, Silverstein FS, Johnston MV. MK-801 protects the neonatal brain from hypoxic–ischemic damage. Eur J Pharmacol 1987;140:359–61.
[51] Dalous J, Pansiot J, Pham H, Chatel P, Nadaradja C, D'Agostino I, et al. Use of human umbilical cord blood mononuclear cells to prevent perinatal brain injury: a preclinical study. Stem Cells Dev 2013;22:169–79.
[52] Gao J, Dennis JE, Muzic RF, Lundberg M, Caplan AI. The dynamic in vivo distribution of bone marrow-derived mesenchymal stem cells after infusion. Cells Tissues Organs 2001;169:12–20.
[53] Zhang L, Li Y, Zhang C, Chopp M, Gosiewska A, Hong K. Delayed administration of human umbilical tissue-derived cells improved neurological functional recovery in a rodent model of focal ischemia. Stroke 2011;42:1437–44.
[54] Lee JA, Kim BI, Jo CH, Choi CW, Kim EK, Kim HS, et al. Mesenchymal stem-cell transplantation for hypoxic–ischemic brain injury in neonatal rat model. Pediatr Res 2010;67:42–6.
[55] Fischer UM, Harting MT, Jimenez F, Monzon-Posadas WO, Xue H, Savitz SI, et al. Pulmonary passage is a major obstacle for intravenous stem cell delivery: the pulmonary first-pass effect. Stem Cells Dev 2009;18:683–92.
[56] Schrepfer S, Deuse T, Reichenspurner H, Fischbein MP, Robbins RC, Pelletier MP. Stem cell transplantation: the lung barrier. Transplant Proc 2007;39:573–6.
[57] Barbosa da Fonseca LM, Gutfilen B, Rosado de Castro PH, Battistella V, Goldenberg RC, Kasai-Brunswick T, et al. Migration and homing of bone-marrow mononuclear cells in chronic ischemic stroke after intra-arterial injection. Exp Neurol 2010;221:122–8.

RESEARCH ARTICLE

International Journal of Geriatric Psychiatry

Delayed atrophy in posterior cingulate cortex and apathy after stroke

Kiwamu Matsuoka[1], Fumihiko Yasuno[1,2], Akihiko Taguchi[3,4], Akihide Yamamoto[2], Katsufumi Kajimoto[3], Hiroaki Kazui[5], Takashi Kudo[5], Atsuo Sekiyama[6], Soichiro Kitamura[1], Kuniaki Kiuchi[1], Jun Kosaka[1], Toshifumi Kishimoto[1], Hidehiro Iida[2] and Kazuyuki Nagatsuka[3]

[1]Department of Psychiatry, Nara Medical University, Kashihara, Japan
[2]Department of Investigative Radiology, National Cerebral and Cardiovascular Center, Suita, Japan
[3]Department of Neurology, National Cerebral and Cardiovascular Center, Suita, Japan
[4]Institute of Biomedical Research and Innovation, Foundation for Biomedical Research and Innovation, Kobe, Japan
[5]Department of Neuropsychiatry, Osaka University Medical School, Suita, Japan
[6]Department of Brain Science, Osaka City University Graduate School of Medicine, Osaka, Japan
Correspondence to: F. Yasuno, MD, PhD, E-mail: ejm86rp@yahoo.co.jp

Objective: A few studies have been performed on chronic structural changes after stroke. The primary purpose of the present study was to investigate regional cortical volume changes after the onset of stroke and to examine how the cortical volume changes affected neuropsychiatric symptoms.

Methods: Participants were 20 stroke patients and 14 control subjects. T1-MRI was performed twice, once at the subacute stage and again 6 months later, and whole brain voxel-based morphometric (VBM) analysis was used to detect significant cortical gray matter volume changes in patients. We also assessed the correlation between changes in cortical volumes and changes in neuropsychiatric symptoms during the 6 months following a stroke.

Results: In the present study, we found significant volume reductions in the anterior part of the posterior cingulate cortex (PCC) over the 6 months following a stroke by exploratory VBM analysis. We also found that the amount of volume change was significantly correlated with the change in apathy-scale scores during the 6 months poststroke.

Conclusions: The present study suggests that delayed atrophic change is evident in the PCC 6 months after a stroke. There was greater apathetic change in the stroke patients with the larger volume reductions. The delayed atrophy of the PCC may reflect degeneration secondary to neuronal loss due to stroke. Such degeneration might have impaired control of goal-directed behavior, leading to the observed increase in apathy.

Key words: stroke; apathy; magnetic resonance imaging; voxel-based morphometric analysis; posterior cingulate cortex
History: Received 13 May 2014; Accepted 11 July 2014; Published online in Wiley Online Library (wileyonlinelibrary.com)
DOI: 10.1002/gps.4185

Introduction

Stroke is one of the leading contributors to disease burden. A worldwide study in 2010 showed that stroke was the second most prevalent cause of death, representing an estimated 11.1% of all deaths (Lozano *et al.*, 2012). In respect to morbidity, stroke was found to be the fourth leading cause of lost DALYs (disability-adjusted life years) globally in nonpediatric populations (Mukherjee and Patil, 2011). Further, neuropsychiatric symptoms following stroke, such as cognitive impairment, depression and apathy, are associated with excess disability, cognitive impairment, and mortality in stroke patients (Hackett *et al.*, 2005; Pendlebury and Rothwell, 2009; van Dalen *et al.*, 2013).

Evidence concerning stroke has been compiled and is being applied to clinical practice. However, only a few studies on structural changes in the chronic stage

exist. A recent study reported atrophic change in regions anatomically remote from the ischemic lesions (Kraemer *et al.*, 2004), which may reflect degeneration secondary to neuronal loss, possibly Wallerian degeneration. This may mean that degenerative cortical changes appear after an ischemic attack, and that this cortical damage produces a biological vulnerability to neuropsychiatric symptoms after a stroke. However, to our knowledge, there has been no studies that focused on where and how the degenerative cortical changes occurred and whether these affected neuropsychiatric symptoms after a stroke.

The primary purpose of the present study was to investigate regional cortical volume changes after the onset of stroke and to examine how they affected any neuropsychiatric symptoms developing in the patient after the stroke. T1-MRI was performed twice, once at the stage of subacute stroke and again 6 months after the stroke, and whole brain voxel-based morphometric (VBM) analysis was used to quantify cortical gray matter (GM) volume changes in patients during the 6-month period following the stroke. We also assessed the correlation between changes in cortical volumes and any changes in neuropsychiatric symptoms.

We hypothesized that regions, such as cingulate cortex, which have unusually extensive connectivity with other areas, would show especially large degenerative cortical changes in stroke due to simultaneous loss of connections from many spatially distinct sites individually affected by the stroke. The regions of degenerative cortical change might relate to the network abnormalities underlying poststroke depression/apathy, which is a common and serious emotional symptom following stroke.

Methods

Subjects

After the study had been completely described to the subjects, and before enrollment, written informed consent was obtained. The study was approved by the Medical Ethics Committee of the National Cerebral and Cardiovascular Center of Japan. The patients were of Japanese ethnicity and were recruited from the neurology unit of the National Cerebral and Cardiovascular Center hospital. These patients had initially been hospitalized for treatment of acute ischemic stroke.

Stroke is diagnosed by neurologists according to the World Health Organization (WHO) criteria. After the assessment, a group of psychiatrists and neurologists reviewed the data and reached a consensus regarding the presence or absence of psychiatric disease, including dementia, according to DSM-IV criteria. Patients were included if they met the following criteria: (i) a focal lesion of either the right or left hemisphere on MRI; (ii) absence of other neurologic, neurotoxic, or metabolic conditions; (iii) modest ischemic insult (modified Rankin scale ≤ 4) with absence of a significant verbal comprehension deficit; and (iv) occurrence of stroke 10–28 days before the first examinations. Exclusion criteria were the following: (i) transient ischemic attack, cerebral hemorrhage, subdural hematoma, or subarachnoid hemorrhage; (ii) history of a central nervous system disease, such as tumor, trauma, hydrocephalus, Parkinson's disease, etc.; and (iii) any pre-stroke history of depression/apathy. Twenty stroke patients who fulfilled the criteria and completed the series of examinations were included in this study. Fourteen control subjects were recruited who completed a series of examinations for the 6-month follow-up study. Exclusion criterion for the control subjects was a history or present diagnosis of any DSM-IV axis-I or neurological illness.

MRI examinations were conducted twice for all patients and control subjects, once at the subacute stage (10–28 days after onset) and again at the chronic stage (6 months after onset). The lesion location was established from MRI data, and its volume was calculated from a volume of interest manually delineated on the lesion. There were no changes in medication usage between baseline and follow-up, and no patient or control was on antidepressant treatment during the examinations. All patients were subjected to a neurological examination [modified Rankin scale, (mRS) (Brott *et al.*, 1989); National Institutes of Health Stroke Scale, NIHSS (Goldstein and Samsa, 1997)] on the day of the MRI scan. All patients and control subjects were administered a series of standardized, quantitative measurements of depressive symptoms [Zung Self-rating Depression Scale, SDS (Zung, 1965); Apathy scale (Starkstein *et al.*, 1993); and mini-mental state examination (for cognitive function), MMSE (Folstein *et al.*, 1975)] on the day of the MRI scan.

MRI data acquisition

All MRI examinations were performed using a 3.0-Tesla whole-body scanner (Signa Excite HD V12M4; GE Healthcare, Milwaukee, WI, USA) with an 8-channel phased-array brain coil. High-resolution three-dimensional T1-weighted images were acquired using a spoiled gradient-recalled sequence ($TR = 12.8$ ms, $TE = 2.6$ ms, flip angle = 8°, $FOV = 256$ mm; 188 sections in the sagittal plane; acquisition matrix, 256×256; acquired

resolution, $1 \times 1 \times 1$ mm). T2-weighted images were obtained using a fast-spin echo ($TR = 4{,}800$ ms; $TE = 101$ ms; echo train length (ETL) = 8; $FOV = 256$ mm; 74 slices in the transverse plane; acquisition matrix, 160×160, acquired resolution, $1 \times 1 \times 2$ mm).

Image processing

Image preprocessing and statistical analyses were carried out using SPM8 software (Wellcome Department of Imaging, Neuroscience Group, London, UK; http://www.fil.ion.ucl.ac.uk/spm), and VBM was carried out using the VBM8 toolbox (http://dbm.neuro.uni-jena.de/vbm.html) with default parameters. Images were bias-corrected, tissue classified, and registered using linear (12-parameter affine) and nonlinear transformations (warping), within a unified model (Ashburner and Friston, 2005). Subsequently, analyses were performed on GM segments, which were multiplied by the nonlinear components derived from the normalization matrix in order to preserve actual GM values locally (modulated GM volumes). Finally, the modulated volume was smoothed with a Gaussian kernel of 5 mm full-width at half-maximum. The voxel size of the final images was $1.5 \times 1.5 \times 1.5$ mm.

Voxel-wise GM differences before and after a 6-month period beginning shortly after the stroke were examined using paired t-tests. To avoid possible edge effects between different tissue types, we excluded all voxels with GM values of less than 0.2 (absolute threshold masking). As this was a hypothesis-led analysis, we applied a liberal threshold of $p < 0.001$ with an extent of 25 voxels across the whole brain.

Spherical volumes of interest (VOIs) were determined from regions where a significant volume change over the 6-month period was found in patients. The centers of the spherical VOIs were determined from the Montreal Neurological Institute coordinate with peak t-value. The radius of the spherical VOI was determined in accordance with size of the clusters revealed by the analysis. The regional volume was calculated by averaging the values for all voxels within the spherical VOIs.

Statistical analysis

To identify demographic variables distinguishing patients and controls, group differences in demographic characteristics were examined by unpaired t-test and Pearson χ^2-test. To identify changes in neuropsychiatric symptoms and to confirm the SPM8 results on changes in cortical volumes during the first 6 months after a stroke, the psychometric scores and gray matter volumes of spherical VOIs in patients and controls over 6 months were examined by paired t-test. The group differences in changes in the volumes of spherical VOIs over 6 months were examined with repeated-measures analysis of variance.

To examine the relationship between the fractional volume change of VOIs where a significant volume change was found in patients [(volume at 2nd test - volume at 1st test)/volume at 1st test] and the fractional change of depression/apathy scale scores [(scores at 2nd test - scores at 1st test)/scores at 1st test] in patients and controls, we performed Pearson's correlation analysis. Bonferroni correction was applied to avoid type I errors because of the multiplicity of statistical analyses. All statistical tests were 2-tailed and reported at $p < 0.05$. Statistical analysis of the data was performed using SPSS for Windows 21.0 (IBM Japan Inc., Tokyo, Japan).

Results

Demographic and clinical data

Table 1 summarizes the demographic and clinical characteristics of the study subjects. Patients did not differ significantly from controls in age, sex, education, or MMSE scores. On the psychometric scales, patients had worse scores on SDS and apathy scales when compared with controls. Moreover, a history of hypertension was significantly more prevalent in patients than in controls. As shown by the mRS/NIHSS scores, patients showed some disability due to stroke at the time of the initial examination. All of the patients were receiving anticoagulant and/or antiplatelet medication. The mean total volume of infarction was 1.8 ± 1.2 mL.

The locations of the patients' infarctions were restricted to subcortical regions, including the basal ganglia (50.0%), subcortical white matter (40.0%), and thalamus (10.0%). This is because our studies focused on degenerative cortical gray matter changes remote from the primary ischemic lesions therefore, including cases of cortical infarction would make interpretation of the results difficult. In 13 of the patients, the infarction was located in the left hemisphere.

Changes in psychometric scores and regional gray matter volumes over 6 months

As shown in Table 2, we found significant improvement in mRS score, NIHSS score, and MMSE score, while there was no significant change in depression or apathy scale scores overall in patients during the 6 months following the stroke. Two patients at the 1st and one patient

Table 1 Demographic characteristics of patients and control subjects at baseline

Characteristic	Stroke patients ($n=20$)	Control subjects ($n=14$)	t or χ^2	p
Age (y)	69.2 ± 8.5	72.4 ± 3.0	$t=-1.53$	0.14
Female sex (n, %)	4 (20.0)	6 (42.9)	$\chi^2=2.07$	0.15
Education (years)	12.5 ± 3.5	12.3 ± 2.7	$t=0.15$	0.88
MMSE score	27.5 ± 3.4	29.1 ± 1.3	$t=-1.99$	0.06
SDS	27.8 ± 6.1	21.7 ± 1.9	$t=4.17$	<0.001***
Apathy score	9.4 ± 4.0	5.4 ± 4.0	$t=2.84$	0.008**
History of disease, No (%)				
Diabetes mellitus	3 (15.0)	0 (0.0)	$\chi^2=2.30$	0.13
Hyperlipidemia	3 (15.0)	0 (0.0)	$\chi^2=2.30$	0.13
Hypertension	14 (70.0)	1 (0.1)	$\chi^2=13.2$	<0.001**
mRS score	2.1 ± 0.8	—		
NIHSS score	2.5 ± 1.8	—		
Volume of acute infarcts (mL)	1.8 ± 1.2	—		
Acute infarcts (n, %) in:				
Basal ganglia	10 (50.0)	—		
Subcortical white matter	8 (40.0)	—		
Thalamus	2 (10.0)	—		
Laterality of acute hemisphere infarcts				
Left hemisphere (n, %)	13 (65.0)	—		

MMSE, Mini-Mental State examination; SDS, Zung Self-rating Depression Scale; mRS, modified Rankin scale; NIHSS, National Institutes of Health Stroke Scale.
Data are mean ± sd.
*, $p<0.05$;
**, $p<0.01$;
***, $p<0.001$.

Table 2 Changes in psychometry scores and PCC volume over 6 months in patients ($n=20$) and controls ($n=14$)

	10–28 days after stroke	6 months after first exam	paired t-test (t)	p
Patients				
mRS score	2.1 ± 0.8	1.6 ± 0.6	3.68	0.002**
NIHSS score	2.5 ± 1.8	1.0 ± 0.8	4.41	<0.001***
MMSE score	27.5 ± 3.5	28.9 ± 2.1	−2.32	0.03*
SDS	27.8 ± 6.1	28.1 ± 9.8	−0.17	0.87
Apathy score	9.4 ± 4.0	9.4 ± 4.3	−0.05	0.96
Volume of PCC	0.40 ± 0.07	0.38 ± 0.06	5.60	<0.001***
Controls				
MMSE score	29.1 ± 1.3	29.6 ± 0.5	−1.53	0.15
SDS	21.7 ± 1.9	22.2 ± 2.4	−1.20	0.25
Apathy score	5.4 ± 4.0	5.1 ± 3.5	0.64	0.53
Volume of PCC	0.43 ± 0.06	0.43 ± 0.06	−0.44	0.67

mRS, modified Rankin scale; NIHSS, National Institutes of Health Stroke Scale; MMSE, Mini-Mental State examination; SDS, Zung Self-rating Depression Scale; PCC, posterior cingulate cortex.
Data are mean ± sd.
*, $p<0.05$;
**, $p<0.01$;
***, $p<0.001$.

at the 2nd examination had clinically relevant depression (SDS score >=40), while three patients at the 1st and two at the 2nd examination had clinically relevant apathy (apathy scale score >=14). We found no significant changes in MMSE, depression scale, or apathy scores in control subjects over the 6-month study.

Voxel-based analysis revealed a significant reduction in volume of the anterior part of the PCC in the patients 6 months after the stroke [$(x, y, z)=(-3, -10, 33)$, cluster voxel size = 38, $T=4.77$] (Figure 1). The radius of the spherical VOI was determined to be 3 mm, so that the volume of this size of VOI

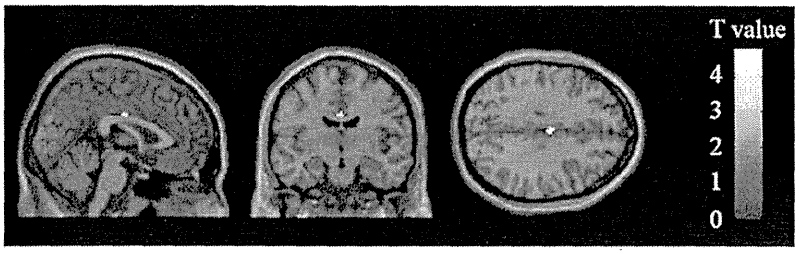

Figure 1 Gray matter volume changes in stroke patients over 6 months, by voxel-based analysis. Images are presented in radiological orientation. Detected areas exceed an uncorrected p-value of 0.001 in 25 or more contiguous voxels. These statistical parametric mapping projections are then superimposed on representative transaxial ($z = 33$), sagittal ($x = -3$), and coronal ($y = -10$) magnetic resonance images.

(113.04 mm^3) almost fit the volume of the cluster (128.25 mm^3). We found a significant reduction of volume of spherical VOIs in the PCC in patients ($p < 0.001$), but not in controls by paired t-test (Table 2; Figure 2). There was no significant difference in VOI volumes between patients and controls at the first examination by unpaired t-test ($t = 1.20$, $p = 0.24$), but the difference became significant after 6 months ($t = 2.36$, $p = 0.024$). We found a significant group effect on the raw volume change in PCC over 6 months by repeated-measures analysis of variance (group-by-volume interaction, $F_{1,32} = 14.2$; $p < 0.001$).

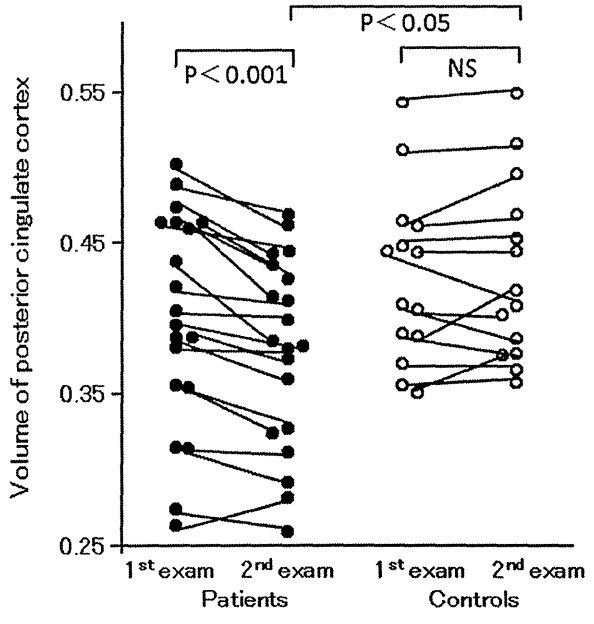

Figure 2 Scatterplots showing volume changes in cingulate cortex over 6 months in patients and controls. We placed spherical VOIs (3-mm radius) on the region where we found significant reduction in volume by voxel-based analysis over 6 months in the patient group. Examining these voxels, we find a significant reduction of gray matter volume in patients ($p < 0.001$) but not in controls by paired t-test. We find a significant group difference in volume only at the 2nd examination.

Relation between volume and apathy scale

We found a significant negative relationship between the fractional change of scored apathy and that of volume change in the PCC VOIs in patients ($r = -0.58$, $p = 0.007$), but not in controls ($r = -0.29$, $p = 0.32$) (Figure 3). When we considered the confounding effects of age, sex, laterality of the infarction, and acute stroke size as covariates in a partial correlation analysis, the above negative relationship remained significant in patients ($r = -0.51$, $p = 0.04$). We found no significant relationships between the fractional change of SDS scores and those of any VOIs in patients or controls.

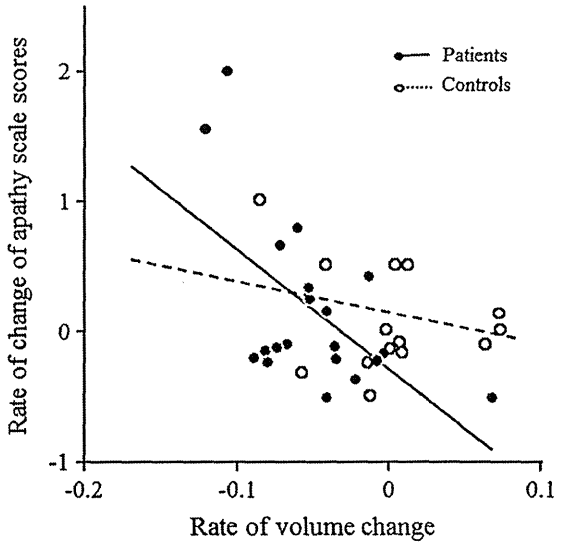

Figure 3 Scatterplots showing the relation between volume change in cingulate cortex and apathy score change over 6 months in patients and controls. A significant correlation is observed between VOI volume change and apathy score change over 6 months in patients ($r = -0.58$, $p = 0.007$), but not in controls ($r = -0.29$, $p = 0.32$) ($y = -9.1 \times x - 0.3$ for patients, $y = -2.6 \times x - 0.1$ for controls). The correlation in patients is still significant after partial correlation analysis with age, sex, laterality of the infarction, and acute stroke size as covariates ($r = -0.51$, $p = 0.04$).

When we divided the patients into two groups whose volume reduction at PCC was less than ($n = 9$) or greater than ($n = 11$) the average (difference in fractional volume change = −0.05), we found a significant difference in the fractional change of scored apathy between the groups (less-than-average group, change = −0.17; greater-than-average group, change = 0.43; $t = 2.41$; $p = 0.03$). When we considered the confounding effects of age, sex, laterality of the infarction, and acute stroke size as covariates in a one-way analysis of covariance the change in the apathy scores between groups showed a trend that did not reach significance ($F_{1, 14} = 3.2, p < 0.1$).

Discussion

In the present study, we found a significant volume reduction in the anterior part of the PCC over the 6 months following a stroke, by exploratory VBM analysis. Furthermore, the fractional volume change was observed to be negatively correlated with the apathy scale scores during the 6 months after the stroke. The reduced volume of PCC due to the 6-month interval was associated with increased apathy scores. Our findings indicate that the neuronal changes in PCC after stroke are one of the factors that affect the degree of poststroke apathy.

In the patients, delayed atrophy was observed in a part of the PCC anatomically remote from the respective subcortical infarct site. This finding may reflect degeneration secondary to neuronal loss, possibly due to Wallerian degeneration, which is a degeneration of distal parts of nerve axons after injury of the proximal axon or cell body (Thomalla *et al.*, 2004). Axonal degeneration, in turn, leads to the death of postsynaptic cell bodies (Raff *et al.*, 2002) and should result in a secondary volume reduction in the part of the brain constituting the projection target of the lost axons. From an anatomical perspective, the PCC has dense structural connections to many other brain regions, suggesting a role as a structural hub (Hagmann *et al.*, 2008). Its volume reduction seen here may reflect the simultaneous loss of multiple afferent projections due to stroke in spatially different sites.

We found more apathetic change in the group of stroke patients with larger volume reductions in PCC. A recent meta-analysis showed that apathy occurred in almost every third patient after a stroke (van Dalen *et al.*, 2013). Because poststroke apathy can have a negative effect on the rehabilitation of activities of daily living or quality of life (Samus *et al.*, 2005; Hama *et al.*, 2007), poststroke apathy has attracted considerable attention. Marin has described apathy as a neuropsychiatric syndrome characterized by diminished goal-directed overt behavior, diminished goal-directed cognition, and diminished emotional concomitants of goal-directed behavior (Marin, 1991).

How is the volume reduction of PCC related to the increase in apathy of stroke patients? The PCC is a hub within the brain, connecting networks that function together to support complex behavior (Hagmann *et al.*, 2008). Leech *et al.* (2011) reported that the PCC is subdivided into dorsal and ventral parts differing in the regions to which they functionally connect. The dorsal part of the PCC is consistent with the region showing the volume reduction in stroke patients in the present study. Anatomically, the dorsal part of the PCC has connectivity with the ventral medial prefrontal cortex, part of the default mode network (DMN), and frontal and parietal regions involved in the cognitive control network (CCN). Abnormalities have been identified in CCN and DMN during episodes of late-life depression that have often been characterized as apathy (Alexopoulos *et al.*, 2012), and the PCC was suggested to have an important role in the regulation of these two networks necessary for controlling efficient goal-directed behavior (Leech *et al.*, 2011). We speculate that the degeneration of the PCC following a stroke might impair the function of control of goal-directed behavior, leading to increased apathy scores.

Our study has some limitations. First, we could not find volume reductions in any other regions of the brain than the PCC. However, the sample size in our study was not large enough to reveal moderate-sized differences between groups. Further study with increased numbers of subjects will be necessary for drawing any definitive conclusions. Second, we could not find associations between cognitive scales and the volume reduction at PCC. We assessed cognitive deficits using MMSE scores, but this test is not highly sensitive to differences between persons with normal and higher performances; thus, the possible presence of a ceiling effect must be considered. Extensive neuropsychological testing is needed for the assessment of cognitive dysfunction. Finally, we were not able to control precisely for important variables, such as social support, premorbid personality, and prior medication histories. Further analysis in light of these points is needed to confirm our present findings.

Conclusion

The present study suggests that delayed atrophic change in the PCC is evident 6 months after a stroke. We also found that the fractional volume change during the 6 months following a stroke was negatively correlated with apathy scale scores. The larger the volume reduction in PCC, the

greater was the increase in apathy-scale scores. The delayed atrophy of part of the PCC seen here may reflect degeneration secondary to neuronal loss due to stroke. Damage in this area may damage control of goal-directed behavior, and it is plausible that such a defect would appear clinically as greater apathy. Knowledge of secondary brain degeneration in stroke patients and its impact on the adverse outcome of development of apathy could provide clues for recognizing new therapeutic targets.

Conflict of interest

None declared.

Key points

- We found significant volume reduction in the anterior part of the PCC over 6 months after the incidence of stroke in patients by exploratory VBM analysis.
- We also found that the rate of volume change was significantly correlated with the apathy scale scores during 6 months post-stroke.
- The delayed atrophy of the PCC may reflect degeneration secondary to neuronal loss due to stroke, and it might deteriorate the function of controlling goal-directed behavior related to apathetic change.

Acknowledgements

We thank the staff of the MRI facility at the Department of Investigative Radiology, National Cerebral and Cardiovascular Center in Japan for subject care and data acquisition during the MRI procedure.

This research was supported by the Japan Society for the Promotion of Science and Grant-in-Aid for Scientific Research (C), 24591740.

References

Alexopoulos GS, Hoptman MJ, Kanellopoulos D, *et al.* 2012. Functional connectivity in the cognitive control network and the default mode network in late-life depression. *J Affect Disord* **139**: 56–65.

Ashburner J, Friston KJ. 2005. Unified segmentation. *Neuroimage* **26**: 839–851.

Brott T, Adams HPJ, Olinger CP, *et al.* 1989. Measurements of acute cerebral infarction: a clinical examination scale. *Stroke* **20**: 864–870.

Folstein MF, Folstein SE, McHugh PR. 1975. "Mini-mental state". A practical method for grading the cognitive state of patients for the clinician. *J Psychiatr Res* **12**: 189–198.

Goldstein LB, Samsa GP. 1997. Reliability of the National Institutes of Health Stroke Scale. Extension to non-neurologists in the context of a clinical trial. *Stroke* **28**: 307–310.

Hackett ML, Yapa C, Parag V, *et al.* 2005. Frequency of depression after stroke: a systematic review of observational studies. *Stroke* **36**: 1330–1340.

Hagmann P, Cammoun L, Gigandet X, *et al.* 2008. Mapping the structural core of human cerebral cortex. *PLoS Biol* **6**: 1479–1493.

Hama S, Yamashita H, Shigenobu M, *et al.* 2007. Depression or apathy and functional recovery after stroke. *Int J Geriatr Psychiatry* **22**: 1046–1051.

Kraemer M, Schormann T, Hagemann G, *et al.* 2004. Delayed shrinkage of the brain after ischemic stroke: preliminary observations with voxel-guided morphometry. *J Neuroimaging* **14**: 265–272.

Leech R, Kamourieh S, Beckmann CF, *et al.* 2011. Fractionating the default mode network: distinct contributions of the ventral and dorsal posterior cingulate cortex to cognitive control. *J Neurosci* **31**: 3217–3224.

Lozano R, Naghavi M, Foreman K, *et al.* 2012. Global and regional mortality from 235 causes of death for 20 age groups in 1990 and 2010: a systematic analysis for the Global Burden of Disease Study 2010. *Lancet* **380**: 2095–2128.

Marin RS. 1991. Apathy: a neuropsychiatric syndrome. *J Neuropsychiatry Clin Neurosci* **3**: 243–254.

Mukherjee D, Patil CG. 2011. Epidemiology and the global burden of stroke. *World Neurosurg* **76**: S85–S90.

Pendlebury ST, Rothwell PM. 2009. Prevalence, incidence, and factors associated with pre-stroke and post-stroke dementia: a systematic review and meta-analysis. *Lancet Neurol* **8**: 1006–1018.

Raff MC, Whitmore AV, Finn JT. 2002. Axonal self-destruction and neurodegeneration. *Science* **296**: 868–871.

Samus QM, Rosenblatt A, Steele C, *et al.* 2005. The association of neuropsychiatric symptoms and environment with quality of life in assisted living residents with dementia. *Gerontologist* **45**: 19–26.

Starkstein SE, Fedoroff JP, Price TR, *et al.* 1993. Apathy following cerebrovascular lesions. *Stroke* **24**: 1625–1630.

Thomalla G, Glauche V, Koch MA, *et al.* 2004. Diffusion tensor imaging detects early Wallerian degeneration of the pyramidal tract after ischemic stroke. *Neuroimage* **22**: 1767–1774.

van Dalen JW, Moll van Charante EP, Nederkoorn PJ, *et al.* 2013. Poststroke apathy. *Stroke* **44**: 851–860.

Zung WW. 1965. A self-rating depression scale. *Arch Gen Psychiatry* **12**: 63–70.

Psychiatry Research: Neuroimaging 223 (2014) 9–14

Contents lists available at ScienceDirect

Psychiatry Research: Neuroimaging

journal homepage: www.elsevier.com/locate/psychresns

Microstructural abnormalities in white matter and their effect on depressive symptoms after stroke

Fumihiko Yasuno [a,b,*], Akihiko Taguchi [c,d], Akihide Yamamoto [b], Katsufumi Kajimoto [c], Hiroaki Kazui [e], Atsuo Sekiyama [f], Kiwamu Matsuoka [a], Soichiro Kitamura [a], Kuniaki Kiuchi [a], Jun Kosaka [a], Toshifumi Kishimoto [a], Hidehiro Iida [b], Kazuyuki Nagatsuka [c]

[a] Department of Psychiatry, Nara Medical University, 840 Shijocho, Kashihara, Nara 634-8522, Japan
[b] Department of Investigative Radiology, National Cerebral and Cardiovascular Center, Suita, Japan
[c] Department of Neurology, National Cerebral and Cardiovascular Center, Suita, Japan
[d] Institute of Biomedical Research and Innovation, Foundation for Biomedical Research and Innovation, Kobe, Japan
[e] Department of Neuropsychiatry, Osaka University Medical School, Suita, Japan
[f] Department of Brain Science, Osaka City University Graduate School of Medicine, Osaka, Japan

ARTICLE INFO

Article history:
Received 11 July 2013
Received in revised form
1 November 2013
Accepted 17 April 2014
Available online 26 April 2014

Keywords:
Stroke
Depression
Magnetic Resonance Imaging (MRI)
Diffusion Tensor Imaging (DTI)
Fractional Anisotropy (FA)
Internal capsule

ABSTRACT

The aim of the study was to investigate the existence of microstructural abnormalities in the white matter of the brain in stroke patients, as well as the relationship between these microstructural abnormalities and changes in depressive symptoms over 6 months. Participants were 29 acute ischemic stroke patients and 37 healthy control subjects. Depressive symptoms were assessed in all subjects using the Hamilton Rating Scale for Depression and the Zung Self-rating Depression Scale. Whole brain voxel-based analysis was used to compare diffusion tensor imaging measures of Fractional Anisotropy (FA) between the groups. Six-month follow-up examinations were conducted. Patients showed significantly lower white matter FA values in the left and right anterior limbs of the internal capsule, and 6 months after the stroke they showed significantly increased FA values in these regions. We found a significant negative correlation between the increased ratio of the FA values and the change in depression scale scores at 6-month follow-up. Regional white matter damage may reflect abnormalities in neuroanatomical pathways related to the pathophysiology of depression.

1. Introduction

Depression is the most common and serious emotional symptom following a stroke and is associated with excess disability, cognitive impairment and mortality (Whyte and Mulsant, 2002). Although there is no consensus about the relationship between lesion location and post-stroke depressive symptoms, Magnetic Resonance Imaging (MRI) studies have found a high prevalence of depressive symptoms in patients with lesions that affect structures of the prefronto-subcortical circuit (Vataja et al., 2001, 2004). Recent studies have highlighted the specific relevance of the Limbic-Cortical-Striatal-Pallidal-Thalamic (LCSPT) circuit in the pathophysiology of major depressive disorder (Drevets et al., 2008; Hasler et al., 2008) and of depression due to stroke (Terroni et al., 2011; Paradiso et al., 2013).

Diffusion Tensor Imaging (DTI) combines a conventional MRI sequence with additional magnetic field gradients to quantify water diffusion, namely, Fractional Anisotropy (FA), the degree to which diffusion is directionally hindered, which reflects the microstructural integrity of the white matter tracts. Microstructural damage to white matter tracts may confer a biological vulnerability to the onset of depressive symptoms in stroke patients. To our knowledge, however, no studies have investigated the existence of microstructural abnormalities of white matter in stroke patients and examined whether the diminution of microstructural abnormalities decreased the vulnerability to post-stroke depression, as measured by increases in depression scale scores in stroke patients that are noted before the onset of severe depression.

Thus, the primary aim of the present study was to investigate the existence of microstructural abnormalities in white matter tracts in stroke patients, as well as the relationship between the recovery from these microstructure abnormalities and the change in depression scale scores 6 months after a stroke. DTI was performed and whole brain voxel-based analysis was used to compare FA between groups of acute ischemic stroke patients

* Corresponding author at: Department of Psychiatry, Nara Medical University, 840 Shijocho, Kashihara, Nara 634-8522, Japan. Tel.: +81 744 22 3051; fax: +81 744 22 3854.
E-mail address: ejm86rp@yahoo.co.jp (F. Yasuno).

http://dx.doi.org/10.1016/j.pscychresns.2014.04.009
0925-4927/

and healthy control subjects. Six-month follow-up examinations were conducted. On the day of the MRI scan, depressive symptoms were evaluated with the Hamilton Rating Scale for Depression and the Zung Self-rating Depression Scale.

2. Methods

2.1. Participants

After complete description of the study to the subjects, written informed consent was obtained. The study was approved by the medical ethics committee of the National Cerebral and Cardiovascular Center in Japan. The patients were of Japanese ethnicity and were recruited from the neurology unit of the National Cerebral and Cardiovascular Center hospital. These patients had initially been hospitalized for treatment of acute ischemic stroke.

Stroke was diagnosed by neurologists according to World Health Organization (WHO) criteria. After the assessment, a group of psychiatrists and neurologists reviewed the data and reached a consensus regarding the presence or absence of psychiatric disease, including dementia, according to DSM-IV criteria. Patients were included if they met the following criteria: (1) a focal lesion of either the right or left hemisphere on MRI; (2) absence of other neurological, neurotoxic, or metabolic conditions; (3) modest ischemic insult (modified Rankin scale ≤ 4) with absence of a significant verbal comprehension deficit; and (4) occurrence of stroke 10–28 days before the examinations. Exclusion criteria were as follows: (1) transient ischemic attack, cerebral hemorrhage, subdural hematoma or subarachnoid hemorrhage; (2) history of a Central Nervous System (CNS) disease such as tumor, trauma, hydrocephalus, and Parkinson's disease; and (3) pre-stroke history of depression. Thirty-eight patients who volunteered to participate in the study were screened for eligibility. We excluded 5 subjects who did not meet the study criteria. In addition, four patients had not completed the MRI scan due to fatigue. A final group of 29 patients met the criteria and participated in this study.

Thirty seven healthy volunteers were recruited from the local area by poster advertisement. Exclusion criteria for the volunteers were a history or present diagnosis of any DSM-IV axis I or any neurological illness. Major characteristics of this cohort are summarized in Table 1. To reliably elucidate differences in white matter integrity between groups, the target total sample size was set at above 52, which was expected to yield power ≥ 0.8, based on $\alpha \leq 0.05$ and assuming a large effect size ($f=0.4$) with the analysis of covariance (ANCOVA) used in this study (Cohen, 1977), and the sample size of this study met the power requirement.

All patients and volunteers were assessed with a series of standardized, quantitative measurements of depressive symptoms [Hamilton Rating Scale for Depression (HAM-D) (Hamilton, 1960), Zung Self-rating Depression Scale (SDS) (Zung, 1965)] and cognitive function [Mini-Mental State examination (MMSE) (Folstein et al., 1975)] on the day of the MRI scan. A neurological examination [modified Rankin scale: mRS (Brott et al., 1989)] was also carried out in the patients. MRIs were conducted for all of the subjects.

Six-month follow-up MRI examinations were also conducted for 18 of 29 patients and 19 of 37 healthy subjects. The other patients and controls were lost to follow-up because we were unable to contact them at 6 months after the first study or they declined to further participate in this study due to health problems, business, feeling of rejection, and so on. On the day of the follow-up MRI scan, the participants underwent the same battery of depressive, cognitive function and (for the patients) neurological measurements that had been performed at the time of the initial MRI. There were no changes in medication between baseline and follow-up. No patients and healthy subjects were diagnosed as meeting DSM-IV criteria for major depression on the day of the initial MRI. Two patients were diagnosed as meeting criteria for major depression for the first time on the day of the follow-up MRI, and they were prescribed medication after the examinations. No patients were on antidepressant treatment during the examinations.

2.2. MRI acquisition

All MRI examinations were performed using a 3-T whole-body scanner (Signa Excite HD V12M4; GE Healthcare, Milwaukee, WI, USA) with an eight-channel phased-array brain coil. DT images were acquired with a locally modified single-shot Echo-Planar Imaging (EPI) sequence by using parallel acquisition at a reduction (ASSET) factor of 2, in the axial plane. Imaging parameters were as follows: repetition time (TR)=17 s; echo time (TE)=72 ms; b=0, 1000 s/mm^2; acquisition matrix, 128 × 128; field of view (FOV), 256 mm; section thickness, 2.0 mm; no intersection gap; 74 sections. The reconstruction matrix was the same as the acquisition matrix, and 2 mm × 2 mm × 2 mm isotropic voxel data were obtained. Motion Probing Gradient (MPG) was applied in 55 directions, the number of images was 4144, and the acquisition time was 15 min, 52 s.

To reduce blurring and signal loss arising from field inhomogeneity, an automated high-order shimming method based on spiral acquisitions (Kim et al., 2002) was used before acquiring DTI scans. To correct for motion and distortion from eddy current and B0 inhomogeneity, FMRIB software (FMRIB Center, Department of Clinical Neurology, University of Oxford, Oxford, England; http://www.fmrib.ox.ac.uk/fsl/) was used. B0 field mapping data were also acquired with the echo time shift (of 2.237 ms) method based on two gradient echo sequences.

High-resolution three-dimensional T1-weighted images were acquired using a spoiled gradient-recalled sequence (TR=12.8 ms, TE=2.6 ms, flip angle=8°, FOV, 256 mm; 188 sections in the sagittal plane; acquisition matrix, 256 × 256; acquired resolution, 1 × 1 × 1 mm). T2-weighted images were obtained using a fast-spin echo (TR=4800 ms; TE=101 ms; echo train length (ETL)=8; FOV=256 mm; 74 slices in the transverse plane; acquisition matrix, 160 × 160, acquired resolution, 1 × 1 × 2 mm).

Table 1
Demographic characteristics of patients and healthy control subjects.

Characteristic	Stroke patients (n=29)	Healthy controls (n=37)	t_{64} or X^2	P
Age (years)	68.7 ± 8.2	67.5 ± 5.2	t=0.77	0.45
Female sex (n, %)	6 (20.7)	15 (40.5)	χ^2=2.95	0.10
MMSE score	27.8 ± 3.0	29.2 ± 1.0	t=2.45	0.02*
SDS score	26.5 ± 5.6	24.1 ± 3.6	t=2.03	0.05*
HAM-D score	2.6 ± 2.5	1.1 ± 1.8	t=2.64	0.01*
mRS score	2.2 ± 0.8	–		
Number of acute infarcts	1.2 ± 0.6	–		
Volume of acute infarcts (ml)	2.0 ± 2.3	–		
Acute infarcts (n, %) in				
Frontal cortex	1 (3.4)	–		
Occipital cortex	1 (3.4)	–		
Basal ganglia	13 (44.8)	–		
Thalamus	4 (13.8)	–		
Subcortical white matter infarcts in				
Frontal lobe	6 (20.7)	–		
Parietal lobe	1 (3.4)	–		
Temporal lobe	1 (3.4)	–		
Occipital lobe	1 (3.4)	–		
Genu of internal capsule	1 (3.4)	–		
Total	10 (34.5)	–		
Laterality of acute hemisphere infarcts				
Left hemisphere (n, %)	17 (58.6)	–		

MMSE=Mini-Mental State Examination. SDS=Zung Self-Rating Depression Scale. HAM-D=Hamilton Rating Scale for Depression. DWMH= deep white matter hyperintensity. PVH=Periventricular hyperintensity. mRS=Modified Rankin Scale. Data are mean ± S.D. * $p < 0.05$.

2.3. Image processing

FMRIB software was used to generate FA maps and three eigenvalues ($\lambda 1$, $\lambda 2$, and $\lambda 3$) from each individual. First, brain tissue was extracted using the Brain Extraction Tool in FSL software. Brain maps for each of the 55 directions were eddy-corrected, subsequent to which FA values were calculated at each voxel using the FSL FMRIB Diffusion Toolbox.

Image preprocessing and statistical analysis were carried out using SPM8 software (Wellcome Department of Imaging Neuroscience, London, England). Each subject's echo planar image was spatially normalized to the Montreal Neurological Institute echo planar image template using parameters determined from the normalization of the image with a b value of 0 s/mm^2 and the echo planar image template in SPM8. Images were resampled with a final voxel size of 2 × 2 × 2 mm^3. Normalized maps were spatially smoothed using an isotropic Gaussian filter (8-mm full-width at half-maximum).

2.4. Voxel-based analysis

Voxel-based analysis was performed using SPM8 software. FA maps were compared between patients and healthy subjects by ANCOVA with age and gender as covariates of no interest. We included age and gender as covariates because it has been reported that they affect the white matter integrity (Inano et al., 2011). Statistical inference was done with a voxel-level threshold of $p < 0.05$, after family-wise error correction for multiple comparisons, with a minimum cluster size of 50 voxels. The regional FA value was calculated by averaging the FA values for all voxels within the voxel of interest (VOI) corresponding to the cluster composed of

significant contiguous voxels in the above analysis. The same VOIs were applied to $\lambda_1-\lambda_3$ images, and $\lambda_1-\lambda_3$ values were extracted. Axial (λ_1) and radial diffusivity ($[\lambda_2+\lambda_3]/2$) were compared.

2.5. Statistical analysis

Group differences in demographic characteristics between patients and healthy controls were examined by unpaired *t*-test and Pearson χ^2 test. To examine the group differences of FA values and axial/radial diffusivity in VOIs shown in the voxel-based analysis, we performed ANCOVA with age and gender as covariates. We included age and gender as covariates because they reportedly affect white matter integrity (Inano et al., 2011). Paired *t*-tests were performed to examine the changes in the mRS, MMSE, SDS, and HAM-D scores and the FA values of patients and controls during the 6-month period after their initial examinations. We computed Pearson's correlations to examine the relationship between FA values and depressive symptoms at the first assessment and at the 6-month follow-up assessment. Pearson's correlations were also used to examine the relationship between the change in depression scale scores and the ratio of the FA values (FA values at second vs. initial examination) in patients. To examine whether the ratio of the FA values was related to the change in depression scale scores (SDS and HAM-D scores at second minus initial examination), we performed a multiple regression analysis with the change in depression scale scores as the dependent variable and the ratio of the FA values as the independent variable, after adjustment for age and gender.

All statistical tests were 2-tailed and reported at $\alpha < 0.05$. Bonferroni correction was applied to avoid type I errors due to the multiplicity of statistical analyses. Statistical analysis of the data was performed using SPSS for Windows 19.0 (IBM Japan Inc., Tokyo, Japan).

3. Results

3.1. Demographic and clinical data

Table 1 summarizes the demographic and clinical characteristics of the participants. Patients differed significantly from healthy control subjects in MMSE, SDS and HAM-D scores. The MMSE score was lower, and SDS and HAM-D scores were higher, among the patients. Table 1 also shows the mRS score and the location and volume of the infarctions among the patients. The main locations of the infarctions were the basal ganglia (44.8%), the subcortical white matter in the frontal lobe (20.7%), and the thalamus (13.8%).

3.2. Between-group comparisons of FA values

In the voxel-based analysis of FA values, the patient and healthy control groups differed in white matter FA values in the left and right anterior limbs of the internal capsule [left anterior limb of internal capsule: $(x, y, z)=(-24, 16, 16)$, cluster voxel size=189, $T=6.41$; right anterior limb of internal capsule: $(x, y, z)=(16, 6, 10)$, cluster voxel size=756, $T=6.86$] (Fig. 1a). Table 2 shows the quantification of the differences in FA value and radial/axial diffusivity in these affected regions. These regions revealed decreased axial diffusivity but no change in radial diffusivity. When we added the MMSE, SDS, and HAM-D scores as covariates in the ANCOVA, the results did not change.

3.3. Change in FA values of patients over 6 months

There were no significant differences in demographic data between participants who were followed and those who were lost to follow-up, except the age of the healthy control groups (Table 3). Table 4 shows the changes in psychometric scores and FA values and axial/radial diffusivity over 6 months in the followed-up patients and controls. Healthy controls showed no significant change of FA values in the anterior limb of the internal capsule 6 months after the initial examination (Table 4). Patients showed significantly increased FA values in the anterior limb of the internal capsule 6 months after the infarction, although their FA values were still lower relative to those of healthy control subjects at this time point (Table 4, Fig. 1b). There were no significant changes in MMSE, SDS and HAM-D scores 6 months after the initial examination in the groups of patients and healthy controls (Table 4).

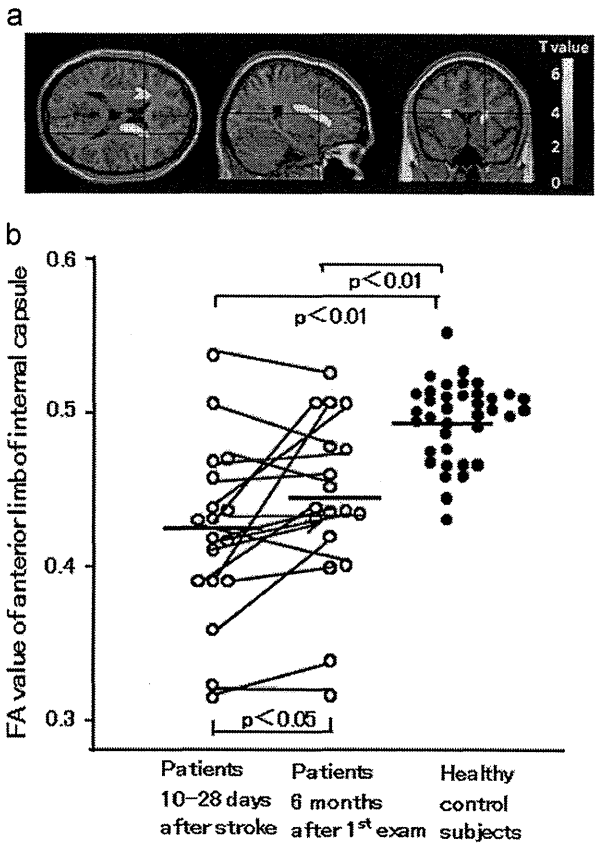

Fig. 1. White matter Fractional Anisotropy (FA) differences in voxel-based comparisons between stroke patients ($n=29$) and control subjects ($n=37$) (Fig. 1a), and scatter plots of FA values in the region of FA reduction among stroke patients ($n=18$) at 10–28 days after stroke/after 6-month follow-up and of control subjects ($n=37$) (Fig. 1b). (a) Images are presented in radiological orientation. Statistical parametric mapping projections were superimposed on a representative magnetic resonance image ($x=24, y=16, z=16$). Patients showed reduced FA in the right and left anterior limbs of the internal capsule. Statistical inferences were made with a voxel-level statistical threshold ($p<0.05$) after family-wise error correction for multiple comparisons with a minimum cluster size of 50 voxels. (b) Significant increase in FA of the patients was observed at 6-month follow-up ($p<0.05$), although the FA values of the patients were still lower than those of healthy subjects at both the initial and follow-up examinations ($p<0.01$).

There were no significant relationships between FA values and depressive symptoms at the first assessment and at the assessment performed 6 months later, but we found a significant negative correlation between the increased ratio of the FA values and the change in the depression scores on the SDS and HAM-D at 6-month follow-up ($r=-0.59$, $p=0.01$ for SDS; $r=-0.56$, $p=0.02$ for HAM-D) (Fig. 2). With Spearman's correlational analysis, the results were not changed ($r=-0.56$, $p=0.02$ for the SDS; $r=-0.73$, $p=0.001$ for the HAM-D). When we considered the influence of the volume of infarcts and lesion location [cortex ($n=2$), basal ganglia ($n=8$), thalamus ($n=1$), and subcortical white matter ($n=7$)] as a covariate in correlational analysis, the correlations were not changed ($r=-0.59$, $p=0.02$ for SDS; $r=-0.57$, $p=0.02$ for HAM-D). When we considered the influence of the degree of handicap by including the change in mRS scores as a covariate in the correlation analysis, which showed a significant decrease during follow-up (mRS score=2.1 ± 0.8 at first examination, 1.6 ± 0.6 at 6-month follow-up, $t=4.12$, $p<0.01$, paired

Table 2
Differences in values of FA and axial/radial diffusivity in VOIs between patients and healthy control subjects.

FA and axial/radial diffusivity	Patients ($n=29$)	Healthy controls ($n=37$)	Analysis of covariance [a]	
			$F(1, 62)$	P
Left anterior limb of internal capsule				
FA	0.44 ± 0.05	0.49 ± 0.05	16.7	$< 0.001^{**}$
Axial diffusivity ($\times 10^{-3}$)	4.16 ± 0.36	4.37 ± 0.35	5.46	0.02^{*}
Radial diffusivity ($\times 10^{-3}$)	3.94 ± 0.33	4.03 ± 0.33	1.38	0.25
Right anterior limb of internal capsule				
FA	0.45 ± 0.05	0.51 ± 0.05	21.8	$< 0.001^{**}$
Axial diffusivity ($\times 10^{-3}$)	4.15 ± 0.36	4.36 ± 0.36	5.19	0.03^{*}
Radial diffusivity ($\times 10^{-3}$)	3.91 ± 0.33	4.01 ± 0.33	1.38	0.24
Average of right and left anterior limbs of internal capsule				
FA	0.44 ± 0.05	0.50 ± 0.05	20.8	$< 0.001^{**}$
Axial diffusivity ($\times 10^{-3}$)	4.15 ± 0.36	4.36 ± 0.35	5.35	0.02^{*}
Radial diffusivity ($\times 10^{-3}$)	3.92 ± 0.33	4.02 ± 0.33	1.38	0.24

Data are mean $\pm$ S.D.

[a] Age and gender are entered as covariates.

* $p < 0.05$.

** $p < 0.01$.

Table 3
Demographic characteristics of patients and healthy control subjects who could be followed up and who were lost to follow-up.

	Follow-up	Lost to follow-up	t or χ^2	P
Patients	$n=18$	$n=11$		
Age (years)	69.2 ± 8.0	67.6 ± 9.0	0.58	0.57
Female sex (n, %)	5 (26.3)	1 (9.1)	1.45	0.24
mRS score	2.1 ± 0.8	2.4 ± 0.9	1.00	0.33
MMSE score	27.6 ± 3.5	27.5 ± 2.8	0.47	0.64
SDS score	26.9 ± 5.6	27.1 ± 7.3	0.42	0.68
HAM-D score	3.1 ± 2.7	2.3 ± 3.0	0.46	0.65
Controls	$n=19$	$n=18$		
Age (years)	69.1 ± 8.0	65.8 ± 8.1	5.22	< 0.01
Female sex (n, %)	10 (55.5)	10 (55.5)	0.03	0.86
MMSE score	29.2 ± 1.2	29.2 ± 0.8	0.10	0.92
SDS score	22.1 ± 1.8	26.2 ± 1.8	1.64	0.11
HAM-D score	0.4 ± 0.6	1.8 ± 2.1	1.61	0.12

t-test), the correlational results were unchanged ($r=-0.61$, $p=0.01$ for the SDS; $r=-0.58$, $p=0.02$ for the HAM-D).

With multiple regression analysis evaluating whether the increased ratio of FA values was related to the change in the SDS and HAM-D depression scores at 6-month follow-up, the ratio of FA values was negatively related to both the changes in the SDS scores (beta$=-0.44$, $p=0.03$) and the HAM-D scores (beta$=-0.46$, $p=0.04$).

4. Discussion

Our findings showed that stroke patients had lower FA in the bilateral anterior limbs of the internal capsule relative to healthy control subjects. Six months after onset, a significant increase in FA was noted, and it was associated with a reduction in depression scale scores. The association of the increase in FA and the reduction in depression scale scores remained significant when we considered the influence of the volume of infarcts and lesion location and the severity of neurological symptoms as a covariate in the partial correlation analysis.

The reduced FA level of patients was associated with decreased axial diffusivity. Axonal damage leads to a marked decrease in axial diffusivity, while demyelination leads to an increase in radial diffusivity (Song et al., 2005). Therefore, our finding was not a result of demyelination but rather of gross reduction in axonal number and/or size, possibly reflecting Wallerian degeneration secondary to neuronal loss due to stroke (Thomalla et al., 2004). From an anatomical perspective, the anterior limb of the internal capsule represents the intercept point in the course of the frontal-subcortical circuits (Axer and Keyserlingk, 2000), and it has extensive connectivity with the cortical and subcortical areas. Its reduced FA may reflect the conjunctive focus of degeneration due to stroke in spatially different sites of cortical and subcortical areas.

The frontal-striatal-thalamic-cortical circuits play an important role in behavioral regulation (Duran et al., 2009), and microstructural change in the anterior limb of the internal capsule was shown to be related to the severity of depressive symptoms in adults with Major Depressive Disorder (MDD) using MRI (Zou et al., 2008). Degeneration in this region may relate to a loss of white matter integrity of these neural circuits (Budde et al., 2007), and this abnormality might trigger the onset of negative mood change. Our finding of a significant negative correlation between the increased ratio of FA values and the change in the depression scale scores 6 months after the stroke might reflect the association between axonal damage of the internal capsule and the negative mood change in stroke patients, and it indicated that recovery from microstructural abnormalities decreased the vulnerability to post-stroke depression, as predicted by elevated depression scale scores.

Our study has some limitations. First, the sample size was not large enough to elucidate the moderate size of difference between groups, and further study with increased numbers of subjects is necessary to draw any definitive conclusions. Second, the stroke patients had predominantly suffered a modest ischemic insult. The extent to which our findings are related to the severity of the ischemic insult was uncertain. Third, patients with significant comprehension deficits were excluded because clinical verbal interviews could not be conducted. Finally, we were not able to control precisely for important variables such as social support, pre-morbid personality, and concurrent and past medication histories. Further analysis, inclusive of consideration of these points, is needed to confirm our present findings.

In conclusion, the present study suggests that FA reduction in the bilateral anterior limbs of the internal capsule is evident in stroke patients. This regional axonal damage should be related to abnormality of neuroanatomical pathways in frontal-subcortical circuits, recent studies of which have highlighted the specific relevance in the pathophysiology of depression due to stroke (Terroni et al., 2011; Paradiso et al., 2013), and it may increase